HHS Public Access

Author manuscript

Free Radic Biol Med. Author manuscript; available in PMC 2017 June 01.

Published in final edited form as:

Free Radic Biol Med. 2016 June ; 95: 308–322. doi:10.1016/j.freeradbiomed.2016.03.031.

Synergistic effects of ascorbate and sorafenib in hepatocellular carcinoma: New insights into ascorbate cytotoxicity

Lauren Rouleau[#1], **Anil Noronha Antony**[#1], **Sara Bisetto**[1], **Andrew Newberg**[3], **Cataldo Doria**[4], **Mark Levine**[2], **Daniel A. Monti**[3,**], and **Jan B. Hoek**[1,**]

[1]MitoCare Center, Department of Pathology, Anatomy and Cell Biology, Thomas Jefferson University, Philadelphia, PA 19107, USA.

[2]Molecular and Clinical Nutrition Section, Digestive Diseases Branch, National Institute of Diabetes and Digestive and Kidney Diseases, Bethesda, MD 20892, USA

[3]Jefferson-Myrna Brind Center of Integrative Medicine, Thomas Jefferson University Hospital, Philadelphia, PA 19107, USA

[4]Division of Transplantation, Liver Tumor Center, Thomas Jefferson University Hospital, Philadelphia, PA 19107, USA

[#] These authors contributed equally to this work.

Abstract

We investigated the mechanism of selective ascorbate-induced cytotoxicity in tumor cells, including Hep G2 cells, compared to primary hepatocytes. H_2O_2 formation was required for ascorbate cytotoxicity, as extracellular catalase treatment protected tumor cells. H_2O_2 generated by glucose oxidase treatment also caused cell killing, but treatment with a pharmacological dose (5-20 mM) of ascorbate was significantly more cytotoxic at comparable rates of H_2O_2 production, suggesting that ascorbate enhanced H_2O_2 cytotoxicity. This was further supported by the finding that ascorbate at a non-cytotoxic dose (1 mM) enhanced cell killing caused by glucose oxidase. Consistent with this conclusion, ascorbate treatment caused deregulation of cellular calcium homeostasis, resulting in massive mitochondrial calcium accumulation. Ascorbate acted synergistically with the chemotherapeutic sorafenib in killing Hep G2 cells, but not primary hepatocytes, suggesting adjuvant ascorbate treatment can broaden sorafenib's therapeutic range. Sorafenib caused mitochondrial depolarization and prevented mitochondrial calcium sequestration. Subsequent ascorbate addition further deregulated cellular calcium homeostasis promoting cell death. Additionally, we present the case of a patient with hepatocellular carcinoma (HCC) who

[*]**Correspondence to:,** Jan B. Hoek, Ph.D., jan.hoek@jefferson.edu, MitoCare Center, Department of Pathology, Anatomy and Cell Biology, Suite 527G JAH, Thomas Jefferson University, 1020 Locust Street, Philadelphia PA 19107, USA. [**] Joint corresponding author.

CONFLICTS OF INTEREST:
The authors declare that there are no conflicts of interest.

had prolonged regression of a rib metastasis upon combination treatment with ascorbate and sorafenib, indicating that these studies have direct clinical relevance.

Keywords

ascorbate; calcium homeostasis; glucose oxidase; hepatocellular carcinoma; Hep G2; hydrogen peroxide; mitochondrial membrane potential; sorafenib; synergy; vitamin C

INTRODUCTION

Hepatocellular carcinoma (HCC) is the second leading cause of cancer death worldwide and the fifth deadliest cancer in men in the United States, with a 5 year survival rate of only 15% (1). HCC is often diagnosed at a late stage, at which point it may be unresectable. The current standard of care for treatment of unresectable HCC is sorafenib (2), a multikinase inhibitor with many targets that include different isoforms of RAF, VEGFR2/3, PDGFR-β, and other receptor and non-receptor tyrosine kinases (3). In HCC, as in many other cancers, the RAF/MEK/ERK pathway may be activated by mutations in RAF or overexpression of receptor tyrosine kinases in the plasma membrane leading to protection from apoptosis and uncontrolled proliferation (4, 5). Apoptosis appears to be a major mechanism of tumor cell killing by sorafenib treatment (6, 7). While sorafenib can stabilize disease, tumor regression is rare and has not been reported with bone metastases (8). In the 2007 SHARP trial, sorafenib produced a survival benefit and mean time to progression of 3 months in patients with Child-Pugh class A liver disease (2). Despite these modest effects, sorafenib is currently the most effective chemotherapeutic option for metastatic HCC. Given the limited treatment options and the significant economic impact of end stage HCC, there is a great need for new and combination therapies (9).

Interest in high-dose ascorbate as a potential cancer treatment stemmed from studies by Cameron and Pauling (10, 11), who reported that treatment with ascorbate increased cancer survival times in some patients. However, these findings could not be reproduced in subsequent double-blind placebo-controlled studies (12, 13). No ascorbate blood concentrations were reported in any of these studies. More recently, interest in ascorbate as an adjuvant in cancer treatment was revived based on pharmacokinetic data from healthy subjects showing that ascorbate concentrations in blood were tightly controlled with oral intake, but this control could be circumvented by intravenous administration to achieve plasma concentrations in humans as high as 30 mM (14-17). In the earlier cancer reports, ascorbate was administered orally in the double-blind studies, but both intravenously and orally in the Cameron-Pauling case series (18). Building on this pharmacology foundation, Chen et al. (19,20) discovered that only pharmacologic ascorbate ([ascorbate] > 1 mM) selectively targeted cancer cells through extracellular production of hydrogen peroxide (H_2O_2) mediated by the ascorbate radical (21). Degradation of extracellular H_2O_2 by addition of catalase abrogated the cytotoxic effects of ascorbate (16, 19, 22). Selective cytotoxicity of pharmacologic ascorbate for tumor cells compared to non-transformed cells was also observed in studies on different cell lines (16, 19). However, the basis for this selectivity has not been adequately resolved.

The clinical efficacy of high-dose ascorbate treatment remains largely unexplored. A previous Phase I study from our group reported that pancreatic cancer patients treated intravenously with high-dose ascorbate appeared to tolerate the treatment well and there was overall decreased tumor burden, but the impact on clinical outcomes remains to be established (23). A recent report by Ma et al (22) indicated that patients with ovarian cancer receiving standard chemotherapy had decreased incidence of adverse side effects from chemotherapy upon intravenous treatment with high-dose ascorbate, although patient survival was not significantly affected (22). Additionally, high-dose ascorbate acted synergistically with standard chemotherapy in tumor cell lines and preclinical models (22, 24, 25).

In this paper, we evaluate the mechanism(s) by which pharmacologic ascorbate selectively affects cell viability in Hep G2 and other tumor cell lines compared to primary hepatocytes. We further demonstrate that pharmacologic ascorbate acts synergistically with the standard of care chemotherapeutic drug sorafenib in killing Hep G2 cells through a mechanism that involves dysregulation of cellular calcium homeostasis. In addition, we present data suggesting the clinical relevance of these findings in a case study of a patient with metastatic HCC.

MATERIALS AND METHODS

Reagents

All cell culture reagents were purchased from Roche, ATCC, Sigma-Aldrich, and Life Technologies.

Hepatocyte isolation and culture

Hepatocytes were isolated from male Sprague-Dawley rats (300-400 g) by collagenase perfusion, as described previously (26). Hepatocytes were counted in a hemocytometer, and viability was determined using the trypan blue exclusion method. Viability was maintained at >90%. Hepatocytes were cultured in Williams's E medium (Sigma-Aldrich) supplemented with 1% newborn calf serum, penicillin-streptomycin solution (100 μg/mL each), 50 μg/mL gentamycin solution,100 nM dexamethasone, and 2 mM glutamine. Cells were cultivated in a humidified 5% CO_2 incubator at 37 °C. All animals were used in accordance with mandated standards of humane care and were approved by the Thomas Jefferson University Institutional Animal Care and Use Committee (protocol number: 00082).

Cell culture and viability assays

Hep G2 cells [HEPG2] (ATCC® HB8065™) were grown in EMEM media containing 10% FBS and penicillin–streptomycin solution (100 μg/mL each). SNU-449 cells (ATCC® CRL2234™) were grown in RPMI media containing 10% FBS and penicillin–streptomycin solution (100 μg/mL each). HuH-7 cells were grown in DMEM media containing 10% FBS, penicillin–streptomycin solution (100 μg/mL each), and MEM non-essential amino acids (Invitrogen 11140050). T47D cells (ATCC® HTB133™) were cultured in RPMI-1640 media, supplemented with 10% fetal bovine serum (FBS), 20 μg/mL bovine insulin (Sigma-Aldrich) and penicillin–streptomycin solution (100 μg/mL each). MIA PaCa2 cells (ATCC®

CRMCRL1420™) were grown in DMEM media containing 20% FBS and penicillin-streptomycin solution (100 μg/mL each). All cells were cultivated in a humidified 5% CO_2 incubator at 37 °C.

Cells were harvested by exposure to 0.25% trypsin-EDTA and seeded into 24 well BD Primaria Plates (BD falcon) at a density of 100,000 cells/well and allowed to attach overnight. If inhibitors were included in the experiment, (3-amino-1,2,4-triazole - 5 mM, BCNU - 100 μM; Sigma), cells were exposed for a 1 hour period prior to ascorbate treatment. If sorafenib (Cayman Chemical 10009644) was used, it was added during initial plating and remained in the media throughout. Ascorbate was dissolved in water and the pH was adjusted to 7.4 using NaOH. The solution was made fresh for each experiment and used within an hour of preparation to prevent excessive oxidation. Ascorbate treatment was performed for 2 hours. All incubations were done in their respective growth media in a humidified 5% CO_2 incubator at 37°C, except for Hep G2 cells which were plated and incubated in RPMI-1640 medium (as opposed to EMEM medium). The cells were then washed twice with PBS and an ATP assay (CellTiter-Glo®) or MTT assay was performed to assess cell viability.

ATP viability assay: The ATP viability assay was performed using CellTiter-Glo® Luminescent Cell Viability Assay (Promega G7570) as per manufacturer's instructions.

MTT assay: Cells were further incubated for an additional 3 hours with media containing the MTT (Thiazolyl Blue Tetrazolium Bromide) reagent (0.5 mg/mL). The MTT formazan product was then dissolved in acid-Isopropanol (1:19 – 1N HCl:Isopropanol) and optical density was measured at 570 nm against background at 630 nm. Viability was calculated as percent of control.

Enzyme activity assays

Whole cell protein lysates were used to determine catalase and glutathione peroxidase (GPX) activity.

Catalase activity was measured spectrophotometrically by the method of Beers and Sizer (27), which monitors the decomposition of peroxide at 240 nm. This is a direct assay with pseudo-first-order kinetics. Catalase activity is calculated using the following expression:

$$\text{Units/mg protein} = (3.45 * df) / (min * 0.1 * (\text{mg protein/mL sample}))$$

The factor 3.45 corresponds to the decomposition of 3.45 μmoles of H_2O_2 in a 3 mL reaction mixture producing a decrease in the A240 nm from 0.45 to 0.40 Absorbance Units (AU); df is the dilution factor; min is the time taken for A240 nm to decrease from 0.45 to 0.40 AU and 0.1 is the volume (in mL) of sample/enzyme used. One unit is defined as the amount of catalase that will decompose 1.0 μmole of H_2O_2 per minute at pH 7.0 at 25°C, while the H_2O_2 concentration falls from 10.3 mM to 9.2 mM.

GPX activity was measured by a coupled assay that relies on the NADPH-dependent reduction of glutathione disulfide (GSSG) formed during the enzymatic reduction of H_2O_2

by GPX. Glutathione reductase reduces the GSSG to glutathione (GSH) using NADPH as the electron donor and GPX activity is measured by the oxidation of NADPH at 340 nm. This is a modification of the assay described by Flohé and Gunzler (28) and was performed as previously described (29). Units of GPX activity are defined as μmole NADPH oxidized per min at the specified GSH concentration, using 6.22 as the millimolar extinction coefficient for NADPH.

H_2O_2 assay

H_2O_2 levels in cell culture medium with or without Hep G2 cells were measured by detecting catalase-dependent O_2 formation, using a Hansatech Oxygraph Plus attached to a 37 °C water bath similar to the method described by Du (30). The oxygen electrode was calibrated with air saturated RPMI-1640 media followed by the addition of sodium dithionite to establish zero oxygen. A calibration curve was generated in 1 mL RPMI-1640 media and 10^4 units of catalase (EC 1.11.1.6, Sigma-Aldrich C3155-50MG) by injecting freshly prepared solutions of H_2O_2 into the chamber using a Hamilton syringe. 1 mL of sample was added to the chamber, obtained from cell cultures treated with ascorbate or glucose oxidase (GOX) (EC 1.1.3.4, Sigma-Aldrich G7141-50KU) at various doses or time points. After a stable baseline was established, catalase was injected into the chamber and O_2 production was recorded. After a stable reading was obtained a known quantity of H_2O_2 of was injected for calibration. For quantitation, O_2 formation was further compared to the H_2O_2 standard curve.

Live cell epifluorescence microscopy

Preparation of coverslips for imaging—All coverslips were prepared in a biosafety cabinet. Coverslips were washed in 200 proof ethanol and allowed to dry. Coverslips were then coated with poly-D-lysine hydrobromide (Sigma-Aldrich P-6407) to assist with attachment. After 15 minutes the poly-D-lysine was removed and coverslips were washed 2 times with sterile water and then exposed to UV light for 30 minutes. Hep G2 cells were trypsinized, counted, and plated on coverslips at a density of 40,000 cells/coverslip and allowed to attach overnight.

Imaging measurements were performed in a 0.25% bovine serum albumin (BSA)–imaging medium (IM) consisting of 121 mM NaCl, 5 mM $NaHCO_3$, 4.7 mM KCl, 1.2 mM KH_2PO_4, 1.2 mM $MgSO_4$, 2 mM $CaCl_2$, 10 mM glucose, and 10 mM Na-Hepes, pH 7.4, at 35°C.

Methods for HyPer/SypHer transfection and analysis by live cell epifluorescence microscopy—HyPer is derived from the OxyR domain of *Escherichia coli,* a selective H_2O_2 sensing protein, which is modified to contain the circularly permuted (cp) YFP fluorophore. The HyPer probe has two excitation peaks (420 and 500 nm) that have opposite fluorescence changes in response to H_2O_2, thereby allowing for ratiometric imaging of the fluorescence signal (which corrects for differences in HyPer expression) to detect changes in intracellular H_2O_2 in the sub- to low micromolar range (31). HyPer can be selectively targeted to the cytosolic space or the mitochondrial matrix and be used to detect H_2O_2 in either of these compartments. $HyPer_{cyto}$ and $HyPer_{mito}$ expression vectors were purchased from Evrogen (FP941 and FP942 respectively). $SypHer_{cyto}$ and $SypHer_{mito}$

expression vectors were originally acquired from Damon Poburko (32). Plasmids were amplified in *Escherichia coli* DH5-Alpha and purified using the Qiagen Plasmid Midi Kit (12143). 2 μg of plasmid was used for the transfection, ratio 1:3 with X-tremeGENE 9 DNA transfection reagent (Roche 06365779001). Cells were transfected 24 hours after attaching to coverslips and imaged 24 hours after transfection. Coverslips were positioned in the imaging chamber with 1 mL of 0.25 % BSA-IM at room temperature and placed on the heated stage (37°C) of an inverted epifluorescence microscope (Olympus) with 40 × oil objective connected to a cooled CCD camera (PXL, Photometrics). Ratiometric imaging was performed at 495 nm and 415 nm (31, 33).

Cellular calcium measurements—Hep G2 cells on coverslips were loaded with 4 μL of 50 μg/μL Fura-2 AM (TEFlabs 0103) for 10 min in the presence of 100 mM sulfinpyrazone and 0.003% (w/v) pluronic acid in 2% BSA-IM at 25°C. Coverslips were positioned in the imaging chamber with 3 mL of 0.25% BSA-IM and placed on the heated stage (37 °C) of an inverted epifluorescence microscope (Olympus) with 40 × oil objective connected to a cooled CCD camera (PXL, Photometrics). Ratiometric imaging of Fura-2 AM (340 nm / 380 nm) was used to monitor $[Ca^{2+}]_{cyto}$ as described previously (34-36). Cytosolic calcium concentrations were calculated using a calibration with 1mM $CaCl_2$ for maximum fluorescence followed by 10mM Tris-EGTA pH 7.5 for minimal fluorescence.

Mitochondrial membrane potential measurements—Hep G2 cells plated on coverslips were loaded with 45 nM tetramethyl rhodamine ethyl ester (TMRE) (Life Technologies T-669) for 10 min in 0.25% BSA-IM at 25°C. After dye loading, the cells were rinsed with 0.25% BSA-IM, and the coverslip was mounted to a heated (37°C) incubator chamber in 3 mL of 0.25% BSA-IM and 5 nM TMRE. Detection of TMRE fluorescence (excitation - 545nm, emission – 630/60nm) was achieved using an inverted epifluorescence microscope (Olympus) with 40 × oil objective connected to a cooled CCD camera (PXL, Photometrics) and used to monitor mitochondrial membrane potential as described previously (37-39).

Statistics

Statistical significance was estimated as the standard error of the mean (SEM) for a minimum of n=3 independent experiments unless otherwise noted. Microscopic fluorescence signals (ratiometric where appropriate) were analyzed using at least 2 separate experiments on different days with n≥15 cells per experiment. The combination index (CI) was analyzed through a serial deletion analysis using the CompuSyn software. P values were calculated using an unpaired Student's *t* test.

RESULTS

Ascorbate induces cytotoxicity in human cancer cell lines, but not in primary rat hepatocytes

Ascorbate-induced cytotoxicity was analyzed in different tumor cell lines (Hep G2, HuH-7, SNU-449 (human hepatocellular carcinoma), T-47D (human breast carcinoma), and MIA PaCa-2 (human pancreatic carcinoma)). Cells were grown overnight in their recommended

growth medium as per ATCC and exposed to varying concentrations of ascorbate (1-20 mM) for a period of 2 hours. Cell viability was tested by Cell Titer Glo cell viability assay (which measures ATP levels) or by the MTT assay (which measures viable cells with active oxidative metabolism) at the end of the 2 hour period, and in some experiments after 24 hours. Fig. 1A and B show the ascorbate-induced loss of cell viability after the 2 hour exposure. It should be noted that the MTT assay requires effective washout of ascorbate to avoid interference with the redox sensitive nature of the assay, which may account for the larger variability of the results. Half-maximal cell killing occurred at ascorbate concentrations in the range of 3-5 mM, depending on the cell line. Importantly, there was no apparent recovery of ATP levels after washing out ascorbate and incubating the cells for a further 24 hours (Supplemental Fig. S1B) indicating that the ATP decline was not due to a temporary increase in ATP utilization and there was no additional cell death during this period. Other hepatocellular carcinoma cell lines tested (HuH-7, SNU-449) were similarly sensitive to these concentrations of ascorbate (Supplemental Fig. S1A).

Primary rat hepatocytes cultured overnight on collagen-coated plates were tested for ascorbate-induced cell killing. Incubation with ascorbate for 2 hours did not affect cell viability over the range of concentrations tested (1-20 mM) (Fig. 1A, B). Further overnight culture following the 2 hour ascorbate treatment did not cause additional cell death (Supplemental Fig. S1C) in agreement with earlier reports that non-transformed cells are not affected by ascorbate treatment *in vitro* (19).

Extracellular H_2O_2 production is necessary but not sufficient to account for ascorbate-induced cytotoxicity

Pharmacologic ascorbate concentrations result in the production of H_2O_2 in the extracellular medium, which previous studies identified as the effector for ascorbate-induced cell killing (19, 20). In agreement with these studies, addition of catalase (100 μg/mL, equivalent to 5000 U/mL) to the culture medium during the 2 hour ascorbate treatment effectively rescued the tumor cell lines from ascorbate-induced cytotoxicity (Fig. 1C). Ascorbate-dependent H_2O_2 formation was measured directly in RPMI 1640 medium in the absence of cells using a Clark oxygen electrode assay (19, 40). As shown in Fig. 2A, H_2O_2 formation at different concentrations of ascorbate over a two-hour period ranged from 10-150 μM. The rate of H_2O_2 formation showed evidence of saturation at higher ascorbate concentrations and maximal ascorbate-dependent cell killing required the presence of serum in the medium (Supplemental Fig. S1D), in agreement with a catalytic role for a serum component, as reported previously (19).

The experiment of Fig. 1C demonstrates that H_2O_2 is required for ascorbate-induced cell killing. In further experiments, we tested whether ascorbate-induced H_2O_2 formation is sufficient to account for its cell killing or whether it exerts additional effects beyond acting as a pro-drug for production of H_2O_2. Glucose oxidase (GOX) catalyzes the oxidation of D-glucose by molecular oxygen to generate H_2O_2 and D-glucono-lactone. GOX-dependent H_2O_2 formation was measured directly in RPMI 1640 medium in the absence of cells using the Clark oxygen electrode assay. As shown in Fig. 2A, net H_2O_2 formation at different concentrations of GOX (1-20 mU/mL) over a two-hour period ranged from 10-400 μM.

GOX at 1-10 mU/mL produced H_2O_2 at a similar rate as that produced by 1-10 mM ascorbate, but without saturation at higher GOX levels. The time course of H_2O_2 accumulation in the cell culture medium over a two hour period was examined in the absence and presence of Hep G2 cells after treatment with either 10 mM ascorbate, 10 mU/mL GOX, 1 mM ascorbate, or 10 mU/ml GOX *plus* 1 mM ascorbate (Figs. 2B-E). Ascorbate (10 mM) produced H_2O_2 at a linear rate during the first 30 min of incubation, but then gradually declined. By contrast, GOX (10 mU/mL) sustained a linear H_2O_2 production rate throughout the 2 hour incubation, resulting in a larger total H_2O_2 formation. However, when Hep G2 cells were present, H_2O_2 accumulation in the medium gradually approached a steady state of approximately 50 μM with either agent, reflecting the balance between the rate of formation and the cellular metabolism of H_2O_2. Interestingly, although 1 mM ascorbate produced H_2O_2 at a detectable rate even in the presence of Hep G2 cells, the addition of 1 mM ascorbate to incubations with GOX did not increase H_2O_2 accumulation over that with GOX alone.

Incubation of Hep G2 cells with GOX (1-20 mU/mL) for 2 hours was cytotoxic to tumor cells (Supplemental Fig. S1E, Fig. 2F). However, at comparable rates of H_2O_2 production, treatment with ascorbate was consistently more cytotoxic to Hep G2 cells than GOX. Cell killing after a 2 hour incubation of Hep G2 cells with 10 mM ascorbate was >90% (Fig. 1A, Fig 2F), whereas GOX at 10 mU/mL killed <50% of the Hep G2 cells despite maintaining a comparable steady state level of H_2O_2 in the medium. These data suggest that ascorbate has additional actions that contribute to cytotoxicity beyond acting as a pro-drug to produce extracellular H_2O_2. This was further confirmed by incubating cells with the combination of 10 mU/ml GOX and 1 mM ascorbate, This concentration of ascorbate, which by itself did not have cytotoxic effects and did not increase H_2O_2 levels above those produced by GOX alone, significantly enhanced the cell killing by GOX (Fig. 2F).

Intracellular H_2O_2 disposal capacity protects against ascorbate-mediated cell killing

Because extracellular H_2O_2 generation by itself did not predict cell killing, we hypothesized that intracellular H_2O_2 disposal was a determinant of ascorbate-mediated cell killing. To test this, we used pharmacologic inhibitors of antioxidant enzymes. Among the major enzymes that inactivate H_2O_2 in cells are catalase, glutathione peroxidase, thioredoxin reductase and peroxiredoxins (41, 42). All isoforms of glutathione reductase and thioredoxin reductase depend on availability of NADPH to maintain the respective cofactors, glutathione and thioredoxin, in the reduced state. As shown in Figs. 3A-C, all cancer cell lines could be further sensitized to pharmacologic ascorbate by inhibiting these intracellular enzymatic activities through preincubation with the catalase inhibitor 3-amino-1,2,4-triazole (AT) or with carmustine (bis-chloroethyl nitrosourea, BCNU), a broad spectrum alkylating agent that serves as an inhibitor of glutathione and thioredoxin reductases (as well as other enzymes affecting thiol redox balance), which prevents the NADPH-dependent reduction of oxidized glutathione or thioredoxin (43,44). Importantly, primary hepatocytes, which are normally resistant to ascorbate-induced cell killing, could be sensitized by treatment with these inhibitors (Fig. 3D).

Given the finding that inhibitors of H_2O_2 disposal potentiated cell killing in both Hep G2 cells and primary hepatocytes, we measured enzymatic activities of catalase and glutathione peroxidase (GPX) in cancer cell lines as compared to normal rat liver and primary rat hepatocytes. Catalase activity in extracts from rat liver tissue and primary rat hepatocytes was one to two orders of magnitude higher than in any of the cancer cell lines (Fig. 3E). Among the cancer cell lines tested, Hep G2 cells had the highest level of catalase activity and expression, which was still 30-fold lower than the activity found in primary hepatocytes and in liver tissue extracts. Also, catalase protein levels detected by Western blotting were markedly higher in rat liver and primary rat hepatocytes than in any of the cancer cell lines (Fig. S2A-B). GPX activity showed analogous results (Fig. 3F) with rat liver tissue lysates and primary rat hepatocytes having a 10-15-fold higher activity than any of the tumor cell lines.

Intracellular H_2O_2 changes in ascorbate and GOX-treated Hep G2 cells

While H_2O_2 formation was linked to ascorbate cytotoxicity, the findings did not account for less efficient cell killing when H_2O_2 was generated by GOX as compared to ascorbate. A possible explanation is that ascorbate, after being transported into the cell, can react with intracellular H_2O_2 leading to formation of short-lived hydroxyl radicals (or other highly unstable cytotoxic reactive oxygen species (ROS)) through the Fenton reaction, provided a source for catalytic Fe^{3+} or other trace metals is available (45). Pharmacologic ascorbate rapidly enters cells, mediated by Na^+-dependent ascorbate transporters SVCT1/2, which saturate at sub-millimolar concentrations of ascorbate (46). Recent evidence suggests that dehydroascorbic acid (oxidized ascorbate) also enters some cancer cells, where it is reduced to ascorbate and mediates cytotoxicity, although prior data are inconsistent (19, 47).

In either case, intracellular H_2O_2 concentrations by themselves may not reliably predict cytotoxicity in a cancer cell line. Under many conditions, even in the absence of extracellular challenges, the mitochondria are both the major source of ROS and a significant target of ROS, as disruption of mitochondrial redox homeostasis can lead to mitochondrial damage and cell death (48-51). To test these possibilities, we compared the increase in intracellular H_2O_2 concentrations in Hep G2 cells induced by pharmacologic ascorbate and by GOX.

Although a multitude of fluorescent probes have been used to detect intracellular ROS levels (52), the majority of these are not selective for H_2O_2 and do not distinguish between this and other forms of ROS. Therefore, we used the genetically encoded ratiometric fluorescent sensor HyPer transfected into Hep G2 cells to elucidate intracellular changes in H_2O_2 levels that precede the onset of cell death (33). The H_2O_2 selectivity of HyPer, as that of its bacterial parent protein OxyR results from the fact that the reactive Cys residue (Cys199 on OxyR) is stabilized in the thiolate form in a hydrophobic pocket that appears to be inaccessible to other oxidants, probably including hydroxyl radicals (53). H_2O_2 oxidizes Cys199 to the sulfenyl form, which leads to a large conformational change and intramolecular disulfide formation in the protein (54), which is detected in the HyPer homolog as a change in YFP fluorescence. As with other ROS-sensing probes, the fluorescence intensity of HyPer is pH sensitive (pKa 8.5). However, a corresponding probe,

SypHer, is available which contains the same cpYFP fluorophore with identical pH sensitivity, but no response to H_2O_2 due to a mutation in one of the active site cysteine residues (32). Therefore, control experiments with targeted SypHer probes allow for a correction of the fluorescence signal due to pH fluctuations to obtain a highly specific H_2O_2 sensor response.

We used the HyPer and SypHer probes to measure intracellular H_2O_2 (see methods). Fig. 4A shows a time course of the live-cell epifluorescence microscopy images of cells expressing cytosolic HyPer ($HyPer_{cyto}$, top two rows) and mitochondrial matrix targeted HyPer ($HyPer_{mito}$, third and fourth row). The top and third rows show the response to ascorbate (10 mM), the second and fourth rows show the response to GOX (10 mU/mL). Initial levels of fluorescence in $HyPer_{cyto}$ transfected cells are somewhat variable, largely reflecting differences in expression level that are corrected for by ratiometric image analysis (all signals normalized to the zero time point). Upon addition of ascorbate or GOX, the majority of cells, after a brief lag phase, show an increase in $HyPer_{cyto}$ fluorescence indicating a rise in cytosolic [H_2O_2]. However, the onset of that increase varied between individual cells (Fig. 4A, top two rows). The selective targeting of the $HyPer_{mito}$ probe to the mitochondrial matrix was evident in the punctate fluorescence pattern in these cells (bottom two rows). Again, addition of either ascorbate (10 mM) or GOX (10 mU/mL) caused an increase in mitochondrial H_2O_2 after an initial lag phase. However, the subsequent change in $HyPer_{mito}$ fluorescence was more uniform, particularly in GOX-treated cells (bottom row). It is also notable that the increase in intracellular H_2O_2 in response to 10 mM ascorbate was less than with 10 mU/mL GOX in both cytosol and mitochondrial matrix, despite the identical extracellular steady state H_2O_2 levels attained with this treatment (Figs. 2B and C).

Figs. 4B-E show the individual cell ratiometric fluorescence traces (in grey) corresponding to the images of Fig. 4A for both the cytosolic and mitochondrial matrix targeted HyPer, in response to treatment with either 10 mM ascorbate (Figs. 4B and D) or 10 mU/mL GOX (Figs. 4C and E). The average of the fluorescence traces for all responsive cells is shown in red. The corresponding responses in SypHer-expressing cells ($SypHer_{cyto}$ or $SypHer_{mito}$) are shown in the Supplemental (Fig. S3). When cells were treated with a cytotoxic concentration of ascorbate (10 mM) or GOX (10 mU/mL), the $HyPer_{cyto}$ and $HyPer_{mito}$ fluorescence signals indicated a delayed increase in H_2O_2 levels detectable after about 5-10 minutes of incubation in both mitochondrial and cytosolic compartments. However, in agreement with the images shown in Fig. 4A, there was a marked cell-to-cell variability, particularly in the $HyPer_{cyto}$ response, with some cells responding early, and often transiently, and other cells showing a delay of 20-40 minutes or longer before an increase in H_2O_2 was detectable, which then accelerated over the subsequent incubation time to reach a steady state response in many cells. Given the sensing range of low micromolar concentrations for HyPer, this suggests that H_2O_2 levels in both compartments had increased towards the upper end of this range. No significant pH changes were detected by the SypHer probes seen in the cytosol or mitochondrial matrix upon ascorbate treatment, although there was a tendency towards a pH decline with GOX treatment (Fig. S3). The variable delay time in responding to a common extracellular H_2O_2 exposure may be partly indicative of cell-to-cell variability in the activity of antioxidant enzymes.

Fig. 4F shows the ratio of the average cytoplasmic HyPer and SypHer fluorescence signals for 1 mM ascorbate, 10 mM ascorbate, or 10 mU/mL GOX treatment, which reflects the averaged pH-corrected changes in $[H_2O_2]_{cyto}$ over time. There was no detectable increase in $[H_2O_2]_{cyto}$ after treatment with 1 mM ascorbate (Fig. S4). The rise in H_2O_2 after treatment with 10 mM ascorbate was slower than and not as pronounced as that after treatment with 10 mU/mL GOX, despite the fact that H_2O_2 formation in the extracellular milieu was comparable under these conditions (Fig. 2B and C). These data highlight the point that the higher rate of cell death in ascorbate-treated Hep G2 cells than in GOX-treated cells occurs despite lower levels of intracellular H_2O_2 accumulation, consistent with the concept that intracellular ascorbate enhances cytotoxicity through mechanisms that are not accounted for by an increase in intracellular H_2O_2, possibly through the efficient reaction of intracellular ascorbate with H_2O_2 to generate hydroxyl radicals through the Fenton reaction.

Cytosolic calcium changes may play a role in ascorbate and GOX-induced cell killing

Given the pivotal role of extracellular H_2O_2 formation in the mechanism of high dose ascorbate cytotoxicity and the close link between ROS and cellular calcium signaling (55, 56), we hypothesized that intracellular calcium homeostasis would be disrupted differently by H_2O_2 generated from pharmacologic ascorbate versus H_2O_2 generated by GOX. To investigate, we monitored changes in cytoplasmic calcium concentration ($[Ca^{2+}_{cyto}]$) with the ratiometric Ca^{2+}-sensitive dye, Fura-2 AM (Fig 5A-D).

The resting $[Ca^{2+}_{cyto}]$ in untreated Hep G2 cells was approximately 100-200 nM and remained stable throughout the incubation period (Fig. 5A). Addition of a maximally effective concentration of the uncoupler carbonyl cyanide-p-trifluoromethoxyphenylhydrazone (FCCP) (5 μM) after 60 minutes incubation caused only a small increase in $[Ca^{2+}_{cyto}]$ (Fig. 5A). This concentration of FCCP is sufficient to depolarize the mitochondria and release matrix calcium into the cytosol. Treatment with 10 mM ascorbate caused a marked, but heterogeneous increase in $[Ca^{2+}_{cyto}]$ in the majority of cells (Fig. 5B). Importantly, when FCCP was added after 60 min incubation with ascorbate, a massive increase in $[Ca^{2+}_{cyto}]$ occurred, likely reflecting the accumulation of calcium in the mitochondrial matrix during the course of ascorbate incubation. Even many of those cells that did not exhibit a large increase in $[Ca^{2+}_{cyto}]$ during ascorbate incubation showed FCCP-induced calcium release. Addition of catalase (100 μg/mL) completely suppressed the ascorbate-induced changes in $[Ca^{2+}_{cyto}]$ indicating its dependence on the formation of extracellular H_2O_2 (Fig. 5D). Notably, the ascorbate-induced change in $[Ca^{2+}_{cyto}]$ in many cells occurred immediately upon addition of ascorbate, at time points before intracellular H_2O_2 was found to increase (Figs. 4B and 5B). Incubation of Hep G2 cells with GOX (10 mU/mL) also showed a significant, though more gradual increase in $[Ca^{2+}_{cyto}]$ with less cell-to-cell variability. Again, FCCP addition after 60 min induced a massive release of mitochondrial calcium indicating the mitochondria are actively taking up calcium (Fig. 5C). Thus, these findings suggest that formation of extracellular H_2O_2 upon treatment with either ascorbate or GOX results in deregulation of cellular calcium homeostasis leading to mitochondrial calcium overload. The patterns of calcium dysregulation were different for pharmacologic ascorbate vs. GOX, again consistent with a distinct role of ascorbate in cytotoxicity.

Mitochondrial membrane potential changes during ascorbate and GOX-induced cell killing

Mitochondrial calcium accumulation serves both as a metabolic signal to regulate energy metabolism and, in excessive amounts, to trigger mitochondrial damage by inner membrane permeabilization and ROS formation, often preceding cell death. Therefore, we measured mitochondrial membrane potential changes in Hep G2 cells during ascorbate and GOX treatment using the fluorescent membrane potential indicator tetramethyl rhodamine ethyl ester (TMRE). TMRE accumulates in energized mitochondria in response to the high membrane potential across the inner mitochondrial membrane and redistributes rapidly upon depolarization (38). As shown in Fig. 5E, Hep G2 cells incubated under standard conditions maintained a stable membrane potential throughout the 60 min incubation period. Addition of FCCP (5 μM) rapidly and completely depolarized mitochondria. Unexpectedly, treatment of the cells with 10 mM ascorbate or 10 mU/mL GOX caused a substantial, but often transient increase in TMRE fluorescence indicating mitochondrial hyperpolarization (Figs. 5F and 5G). Subsequent addition of FCCP again rapidly depolarized the mitochondria indicating that the fluorescence increase was not due to changes in baseline fluorescence. Also, the concentration of TMRE (45 nM) used in these experiments was well below the concentration where mitochondrial accumulation of the probe would quench the fluorescence signal. These hyperpolarization effects are abrogated by the addition of catalase indicating that H_2O_2 is a necessary precipitating factor (Fig. 5H). Thus, these experiments suggest a mechanism by which formation of extracellular H_2O_2 initiates an increase in cytosolic calcium that promotes mitochondrial calcium uptake to activate oxidative metabolism in Hep G2 cells. However, prolonged or excessive calcium accumulation in individual cells induced depolarization, a phenomenon that was more prevalent in ascorbate-treated cells than upon GOX treatment. Again, these observations are consistent with a role of intracellular ascorbate in enhancing cytotoxicity in these cells.

Ascorbate treatment enhances sorafenib-mediated cell killing in Hep G2 cells, but not in primary rat hepatocytes

Standard of care for unresectable hepatocellular carcinoma is Sorafenib, a broad spectrum tyrosine kinase inhibitor which targets several receptor tyrosine kinases (PDGFR, VEGFR) as well as serine-threonine kinases of the RAF family (C-RAF, B-RAF), which are upstream activators of the ERK/MAP kinase cascade important in cell proliferation (57-59). Sorafenib treatment of Hep G2 cells at therapeutically relevant concentrations (2.5-20 μM) caused cell killing over a 20 hour period with an EC_{50} of approximately 10 μM (Fig. 6A). Primary hepatocytes were equally sensitive to sorafenib-induced cell killing (Fig. 6B) measured by Cell Titer Glo luminescent cell viability assay, indicating that the higher antioxidant activity of the primary cells was not protective. We therefore tested to what extent ascorbate treatment could synergize with sorafenib to enhance cell killing. Figs. 6A and 6B depict dose response curves of the effects of ascorbate treatment on Hep G2 cells and primary hepatocytes pretreated with different concentrations of sorafenib (2.5-20 μM). Pharmacologic concentrations of ascorbate notably enhanced the cell death induced by low concentrations of sorafenib and conversely, sorafenib pretreatment shifted the dose-response curve for ascorbate-induced cell killing to the left (Fig. 6A). Notably, primary rat hepatocytes undergo extensive cell death when treated with > 5 μM sorafenib, but cell killing was not enhanced when sorafenib-treated cells were exposed to ascorbate (Fig. 6B),

suggesting that the synergistic effects of ascorbate and sorafenib depend on the pro-oxidant activity of ascorbate.

For a quantitative estimate of synergy we analyzed the cell killing after treatment with a constant ratio of the combination of ascorbate to sorafenib (2.5 mM/2.5 μM, 5 mM/5 μM, etc.) using the Cell Titer Glo luminescent cell viability assay. Isobologram construction and combination index (CI) calculations were done using the method of Chou and Talalay through the CompuSyn software (60). This analysis provides a quantitative estimate of the combined effects of individual agents in comparison to the effects of each agent individually. CI <1 indicates synergy, CI equal to 1 suggests additivity, and CI>1 indicates antagonism. The CIs for treatment with sorafenib and ascorbate were 0.54, 0.69, and 0.89 for EC_{90}, EC_{75}, and EC_{50} respectively (Fig. 6E), confirming that sorafenib and ascorbate show synergism in Hep G2 cell cytotoxicity *in vitro*. The isobologram in Fig. 6C displays these results graphically. Fig. 6D shows a serial deletion analysis completed on the synergy experiments (n=3) in order to produce a 95% confidence interval of the CI estimates. At effect levels above 55%, the CI is significantly below 1.

Sorafenib enhancement of ascorbate-induced cell killing in Hep G2 cells depends on mitochondrial depolarization

In order to assess the mechanism by which sorafenib can enhance the sensitivity to ascorbate-induced cell killing we analyzed cytosolic calcium changes in Hep G2 cells that were pretreated overnight with 5 μM sorafenib, then washed and loaded with appropriate indicators, and subsequently treated with a combination of moderate concentrations of sorafenib (5 μM) and ascorbate (5 mM) or sorafenib alone. In cells treated with sorafenib alone $[Ca^{2+}_{cyto}]$ was maintained in a relatively stable range, apart from a transient early increase (Fig. 7A). Remarkably, upon treatment with the sorafenib-ascorbate combination, following the initial moderate calcium elevation, there was a dramatic increase in $[Ca^{2+}_{cyto}]$ which extended well into the micromolar range until fluorescence was lost from individual cells in a heterogeneous manner (Fig. 7B). The loss of fluorescence probably reflected plasma membrane permeabilization and loss of calcium indicator dye, indicative of the onset of cell death. Addition of the uncoupler FCCP following the phase of rapid $[Ca^{2+}_{cyto}]$ increase did not cause any release of mitochondrial calcium into the cytosol (Supplemental Fig. S5); this was true even in cells that had not yet lost their calcium indicator dye. Thus, it appeared that the addition of sorafenib in combination with ascorbate, as in Fig. 7B prevented mitochondrial calcium accumulation and caused an excessive increase in cytosolic calcium instead. Notably (Supplemental Fig. S6), incubating cells with sorafenib and ascorbate in a nominally calcium-free medium prevented the large ascorbate-induced increase in $[Ca^{2+}_{cyto}]$ and provided protection against the associated cell death, indicating that calcium influx from the extracellular medium is responsible for the dramatic increase in $[Ca^{2+}_{cyto}]$ shown in Fig. 7B.

Figs. 7C and D demonstrate that addition of sorafenib (5 μM) leads to a rapid decline in mitochondrial membrane potential, both with and without the simultaneous addition of ascorbate (5mM). This finding indicates that sorafenib treatment suppresses mitochondrial energy conservation. Sorafenib has been previously reported to inhibit mitochondrial

Complex I activity (61, 62). Importantly, mitochondrial depolarization by sorafenib treatment in the absence of ascorbate did not elicit the calcium increase and cell permeabilization, indicating that ascorbate is required for the dramatic rise in $[Ca^{2+}_{cyto}]$ and the effect of sorafenib treatment and the consequent mitochondrial depolarization is to sensitize the cells to the specific actions of ascorbate (Fig. 7B). Polarized mitochondria appear to serve as a buffer to prevent excessive $[Ca^{2+}_{cyto}]$ increase and thereby protect against cell killing. Thus, the sensitization by sorafenib likely is due to the failure of depolarized mitochondria to buffer the increase in $[Ca^{2+}_{cyto}]$ initiated by ascorbate-induced H_2O_2 formation. Interestingly, the mitochondrial depolarization by sorafenib appeared to be readily reversible (Supplemental Fig. S7B). Overnight incubation of Hep G2 cells with sorafenib (5 μM) followed by incubation with imaging buffer without sorafenib showed that mitochondria are well-polarized, but can be rapidly depolarized again upon re-addition of FCCP to the imaging buffer (Supplemental Fig. S7A).

Case Study: A patient with metastatic tumor regression after treatment with the combination of high-dose ascorbate and sorafenib

As an initial translational step, we report on a patient with histologically confirmed metastatic stage IV HCC who was treated with a combination of intravenous, high-dose ascorbic acid in combination with standard of care therapy of oral sorafenib. The patient was a 61-year-old white male who presented with metastatic disease to the left 8th rib in March 2013, confirmed by biopsy (See Supplementary Material for further details). His medical oncologist determined that the patient was a candidate for standard of care chemotherapy with sorafenib, and referred the patient to our team to additionally receive intravenous ascorbic acid. We treated him with 75 grams of ascorbic acid administered three times per week. He was also concomitantly given sorafenib 400 mg by mouth, twice a day.

On his initial, pre-treatment CT scan, the patient was observed to have a left 8th rib metastasis measuring 74 × 44 mm, along with a 2.8 × 2.2 cm ablation cavity from pre-metastatic treatment in the right lobe of the liver. After his initial 8-week cycle of ascorbic acid and sorafenib, he underwent CT imaging to evaluate his response. Overall, the findings showed stable disease with no change in the cavitary liver lesion and no significant change in the size of the rib metastasis now measuring 74 × 45 mm. He continued on the same regimen for a second 8-week cycle and was re-imaged. This time the rib lesion was markedly smaller, now measuring 43 × 28 mm, again with no change in the liver and no suggestion of additional metastases. He continued on two additional cycles of the combination therapy during which he maintained the improvement in the rib metastasis on CT scan with otherwise stable disease (Fig. 8). After the 5th cycle (40 weeks) there appeared to be a 10-15% progression of the bone mass from the previous scan, so his oncologist took him off study. Of note, although regression of primary tumor from sorafenib alone has been reported, we are aware of no reports of regression of bony metastasis from sorafenib alone.

DISCUSSION

The data in this paper show that ascorbate in pharmacologic concentrations was cytotoxic to Hep G2 hepatoma cells and other tumor cells, but not to primary hepatocytes. As reported

previously, pharmacologic concentrations of ascorbate generate extracellular H_2O_2, which was essential for cell death. Cytotoxicity of ascorbate in primary hepatocytes was suppressed by the capacity of cells to dispose of H_2O_2, as Hep G2 cells and other cancer cells exhibited markedly lower levels of catalase and glutathione peroxidase than hepatocytes isolated from normal liver tissue and inhibition of catalase and glutathione reductase sensitized primary hepatocytes to ascorbate cytotoxicity and increased cytotoxicity of pharmacologic ascorbate in cancer cells. The decreased activity of antioxidant enzymes, including catalase and glutathione peroxidase in different cancer cell types has been reported previously (63) and may be related to the importance of ROS as signaling molecules. Treatment of different cancer cell types with GOX as an H_2O_2 generating system was less cytotoxic than treatment with pharmacologic ascorbate at comparable rates of H_2O_2 generation, indicating that pharmacologic ascorbate had other actions in addition to generation of extracellular peroxide. These may be due to the formation of highly reactive, but short-lived hydroxyl radicals by the Fenton reaction mediated by ascorbate in the presence of H_2O_2 and Fe^{3+} (or other trace metal ions) (64,65). This interpretation was further substantiated by the observation that the addition of 1 mM ascorbate, which by itself was not cytotoxic to the tumor cells, significantly enhanced the cell killing caused by GOX, even though this treatment did not further increase the H_2O_2 concentration in the medium at steady state (Fig. 2). Our experiments do not establish whether these actions of ascorbate occurred in the cell interior or at its surface. The declining rate of extracellular H_2O_2 production over time in incubations with 10 mM ascorbate or, to a lesser extent, with GOX plus 1 mM ascorbate, may reflect its reaction with accumulating H_2O_2 catalyzed by trace concentrations of Fe^{3+} in the medium. Conversely, the finding that intracellular H_2O_2 accumulation, as detected by the H_2O_2 specific probe HyPer, was much lower in incubations with 10 mM ascorbate than with 10 mU/ml GOX (Fig. 4F) despite similar steady state levels of H_2O_2 in the medium, suggests that intracellular ascorbate can also effectively react with H_2O_2. Hydroxyl radicals are extremely short-lived (half-life in the order of nanoseconds) and their targets tend to be diffusion limited. The finding that ascorbate cytotoxicity was associated with dysregulation of cellular calcium homeostasis suggests that plasma membrane calcium influx was accelerated by ascorbate treatment. Indeed, cells were protected from ascorbate cytotoxicity when calcium was omitted from the incubation medium. We hypothesize that the increased net calcium influx may reflect hydroxyl radical-mediated damage to plasma membrane calcium channels allowing their uncontrolled opening, or to the plasma membrane calcium pump (PMCA), which are known to be sensitive to oxidative damage (66). In energetically competent cells, the increased calcium influx caused by incubation with pharmacologic ascorbate and to a lesser extent GOX treatment was largely sequestered in mitochondria. This process may be protective and even accelerate mitochondrial energy metabolism. However, prolonged mitochondrial calcium accumulation in combination with exposure to H_2O_2 or other ROS would predispose them to the permeability transition and cell death.

The cytotoxic effects of ascorbate were synergistic with those exerted by the multikinase inhibitor sorafenib in experiments on Hep G2 cells, but not in primary hepatocytes. This observation is important because it suggests that pharmacologic ascorbate broadens sorafenib's therapeutic range and enhances its efficacy at doses that are clinically better

tolerated. The potential clinical relevance of this finding is indicated by the case study presented here of a patient with undisputable evidence of metastatic HCC with a lesion on the left 8th rib that showed significant regression over five 8-week cycles of combination treatment with intravenous ascorbate and standard of care sorafenib. Importantly, ascorbate infusion was well tolerated and there were no indications of significant negative side effects. This is the first case report with the observation that high dose ascorbate treatment in combination with sorafenib can be effective in reducing metastatic HCC, and it is noted that to our knowledge there are no reported cases of sorafenib alone reducing a bony lesion.

The mechanism by which ascorbate synergized with low dose sorafenib treatment in promoting cell killing highlights the protective role of mitochondrial calcium buffering. The data indicate that a concentration of sorafenib that is only modestly effective in killing cells during overnight incubation, caused marked depolarization of mitochondria, presumably as a result of inhibition of Complex I of the mitochondrial electron transport chain reported by others (61, 62). The resulting inhibition of mitochondrial calcium uptake caused a dramatic ascorbate-induced increase in cytosolic calcium, indicating a breakdown of the mechanisms that maintain cellular calcium homeostasis immediately preceding the onset of cell death.

Other mechanisms by which sorafenib treatment affects cell function may further contribute to the ascorbate-induced cell killing. Sustained inhibition of mitochondrial electron transport and loss of membrane potential could impair mitochondrial antioxidant mechanisms and thereby enhance mitochondrial ROS formation. Also, while ATP formation in Hep G2 cells is primarily dependent on oxidative glycolysis (67), mitochondrial metabolism is required for biosynthesis of other cell constituents, the depletion of which may make cells vulnerable to oxidative stress conditions. Further studies are required to evaluate such mechanisms.

In conclusion, these observations suggest a novel, complex sequence by which pharmacologic ascorbate treatment causes cell death in tumor cells. Our findings highlight the necessity of extracellular peroxide generation as the initiator of cell death. Formation of extracellular H_2O_2 is required, but not sufficient to cause cell killing. At the pharmacologic ascorbate concentrations used in these experiments, accumulation of H_2O_2, in the presence of trace metal ions, may facilitate the ascorbate-mediated Fenton reaction as a source of highly damaging hydroxyl radicals, both on the cell surface and in the cell interior, following uptake of ascorbate through SVCT1 and 2 (ascorbate transporters). Recent evidence suggests that entry of dehydroascorbic acid (oxidized ascorbate) and its intracellular reduction to ascorbate, either through an NADPH-dependent reductive step, or through ascorbate recycling through the mitochondrial electron transport chain (68) may also initiate tumor cell death (47). Although not tested, it is likely that extracellular dehydroascorbic acid formation accompanies extracellular peroxide formation. However, at the pharmacologic concentrations of ascorbate used in these experiments it is likely that its pro-oxidant activity in generating hydroxyl radicals from H_2O_2 remains the predominant mechanism of its cellular effects. Moreover, the lack of mitochondrial polarization in experiments combining ascorbate and sorafenib treatment provides strong evidence that sorafenib suppresses electron transport and prevents mitochondrial energization, which would make ascorbate recycling less likely to contribute to the ascorbate-induced cytotoxicity. In the data presented here, the resulting dysregulation of cellular calcium homeostasis, presumably through effects

on plasma membrane calcium transport systems, elicits an increase in cytosolic calcium, which is largely sequestered in the mitochondrial compartment, from which it can be released by the addition of uncouplers. In this manner, mitochondrial calcium uptake can protect against an excessive increase in $[Ca^{2+}_{cyto}]$ and thereby extend cell survival. In addition, the associated mitochondrial hyperpolarization may serve as an alternative energy source. However, excessive mitochondrial calcium overload in the presence of H_2O_2 may activate the mitochondrial permeability transition and contribute to the cell death induced by ascorbate treatment. When cells are treated with sorafenib, the protective effects of mitochondrial Ca^{2+} uptake are lost and cellular calcium homeostasis is more rapidly and dramatically deregulated upon ascorbate addition leading to plasma membrane permeabilization and cell death.

Supplementary Material

Refer to Web version on PubMed Central for supplementary material.

ACKNOWLEDGMENTS

This project was supported by a generous grant from the Marcus Foundation to DAM and by a grant from the Circle of Light Foundation to DAM. Additional support came from NIH grant R01 AA018873 to JBH. LR received support from NIH Institutional Training grants T32 GM100836 and T32 AA007463. ML was supported by the Intramural Research Program, NIDDK, and NIH. Additionally, we acknowledge John Eisenbrey, PhD for his generous gift of the HuH-7 cell line.

Abbreviations

AA	ascorbic acid
AT	3-amino-1,2,4-triazole
BCNU	bis-chloroethyl nitrosourea
BSA	bovine serum albumin
$[Ca^{2+}_{cyto}]$	cytosolic calcium concentration
CI	combination index
DRI	dose reduction index
EC	effective concentration
FCCP	Carbonyl cyanide-p-trifluoromethoxyphenylhydrazone
GPX	glutathione peroxidase
GOX	glucose oxidase
HCC	hepatocellular carcinoma
MTT	(3-(4,5-Dimethylthiazol-2-yl)-2,5-Diphenyltetrazolium Bromide)
ROS	reactive oxygen species
SVCT	sodium-dependent vitamin C transporter
TMRE	tetramethyl rhodamine ethyl ester

REFERENCES

1. Ferlay J, Soerjomataram I, Ervik M, Dikshit R, Eser S, Mathers C, et al. GLOBOCAN 2012 v1.0, Cancer Incidence and Mortality Worldwide: IARC CancerBase No. 11. 2014
2. Llovet JM, Ricci S, Mazzaferro V, Hilgard P, Gane E, Blanc J, et al. Sorafenib in Advanced Hepatocellular Carcinoma. N Engl J Med. 2008; 359(4):378–390. [PubMed: 18650514]
3. Wilhelm SM. BAY 43-9006 Exhibits Broad Spectrum Oral Antitumor Activity and Targets the RAF/MEK/ERK Pathway and Receptor Tyrosine Kinases Involved in Tumor Progression and Angiogenesis. Cancer Res. 2004; 64(19):7099–7109. [PubMed: 15466206]
4. Chen J, Fujii K, Zhang L, Roberts T, Fu H. Raf-1 promotes cell survival by antagonizing apoptosis signal-regulating kinase 1 through a MEK-ERK independent mechanism. Proc Natl Acad Sci U S A. Jul 3; 2001 98(14):7783–7788. [PubMed: 11427728]
5. Weinstein-Oppenheimer CR, Blalock WL, Steelman LS, Chang F, McCubrey JA. The Raf signal transduction cascade as a target for chemotherapeutic intervention in growth factor-responsive tumors. Pharmacol Ther. Dec; 2000 88(3):229–279. [PubMed: 11337027]
6. Liu L, Cao Y, Chen C, Zhang X, McNabola A, Wilkie D, et al. Sorafenib blocks the RAF/MEK/ERK pathway, inhibits tumor angiogenesis, and induces tumor cell apoptosis in hepatocellular carcinoma model PLC/PRF/5. Cancer Res. Dec 15; 2006 66(24):11851–11858. [PubMed: 17178882]
7. Fernando J, Sancho P, Fernandez-Rodriguez CM, Lledo JL, Caja L, Campbell JS, et al. Sorafenib sensitizes hepatocellular carcinoma cells to physiological apoptotic stimuli. J Cell Physiol. Apr; 2012 227(4):1319–1325. [PubMed: 21604268]
8. Cheng AL, Kang YK, Chen Z, Tsao CJ, Qin S, Kim JS, et al. Efficacy and safety of sorafenib in patients in the Asia-Pacific region with advanced hepatocellular carcinoma: a phase III randomised, double-blind, placebo-controlled trial. Lancet Oncol. Jan; 2009 10(1):25–34. [PubMed: 19095497]
9. Mishra A, Otgonsuren M, Venkatesan C, Afendy M, Erario M, Younossi ZM. The inpatient economic and mortality impact of hepatocellular carcinoma from 2005 to 2009: analysis of the US nationwide inpatient sample. Liver International. 2013; 33(8):1281–1286. [PubMed: 23710596]
10. Cameron E, Pauling L. Supplemental ascorbate in the supportive treatment of cancer: Prolongation of survival times in terminal human cancer. Proc Natl Acad Sci U S A. Oct; 1976 73(10):3685–3689. [PubMed: 1068480]
11. Cameron E, Pauling L. Supplemental ascorbate in the supportive treatment of cancer: reevaluation of prolongation of survival times in terminal human cancer. Proc Natl Acad Sci U S A. Sep; 1978 75(9):4538–4542. [PubMed: 279931]
12. Creagan ET, Moertel CG, O'Fallon JR, Schutt AJ, O'Connell MJ, Rubin J, et al. Failure of high-dose vitamin C (ascorbic acid) therapy to benefit patients with advanced cancer. A controlled trial. N Engl J Med. Sep 27; 1979 301(13):687–690. [PubMed: 384241]
13. Moertel CG, Fleming TR, Creagan ET, Rubin J, O'Connell MJ, Ames MM. High-dose vitamin C versus placebo in the treatment of patients with advanced cancer who have had no prior chemotherapy. A randomized double-blind comparison. N Engl J Med. Jan 17; 1985 312(3):137–141. [PubMed: 3880867]
14. Levine M, Conry-Cantilena C, Wang Y, Welch RW, Washko PW, Dhariwal KR, et al. Vitamin C pharmacokinetics in healthy volunteers: evidence for a recommended dietary allowance. Proc Natl Acad Sci U S A. Apr 16; 1996 93(8):3704–3709. [PubMed: 8623000]
15. Padayatty SJ, Levine M. New insights into the physiology and pharmacology of vitamin C. CMAJ. Feb 6; 2001 164(3):353–355. [PubMed: 11232136]
16. Chen Q, Espey MG, Sun AY, Pooput C, Kirk KL, Krishna MC, et al. Pharmacologic doses of ascorbate act as a prooxidant and decrease growth of aggressive tumor xenografts in mice. Proc Natl Acad Sci U S A. Aug 12; 2008 105(32):11105–11109. [PubMed: 18678913]
17. Padayatty SJ, Sun H, Wang Y, Riordan HD, Hewitt SM, Katz A, et al. Vitamin C pharmacokinetics: implications for oral and intravenous use. Ann Intern Med. Apr 6; 2004 140(7): 533–537. [PubMed: 15068981]
18. Padayatty SJ, Levine M. Reevaluation of ascorbate in cancer treatment: emerging evidence, open minds and serendipity. J Am Coll Nutr. Aug; 2000 19(4):423–425. [PubMed: 10963459]

19. Chen Q, Espey MG, Krishna MC, Mitchell JB, Corpe CP, Buettner GR, et al. Pharmacologic ascorbic acid concentrations selectively kill cancer cells: Action as a pro-drug to deliver hydrogen peroxide to tissues. Proceedings of the National Academy of Sciences. 2005; 102(38):13604–13609.
20. Chen Q, Espey MG, Sun AY, Lee J, Krishna MC, Shacter E, et al. Ascorbate in pharmacologic concentrations selectively generates ascorbate radical and hydrogen peroxide in extracellular fluid in vivo. Proceedings of the National Academy of Sciences. 2007; 104(21):8749–8754.
21. Parrow NL, Leshin JA, Levine M. Parenteral ascorbate as a cancer therapeutic: a reassessment based on pharmacokinetics. Antioxid Redox Signal. Dec 10; 2013 19(17):2141–2156. [PubMed: 23621620]
22. Ma Y, Chapman J, Levine M, Polireddy K, Drisko J, Chen Q. High-dose parenteral ascorbate enhanced chemosensitivity of ovarian cancer and reduced toxicity of chemotherapy. Sci Transl Med. Feb 5.2014 6(222):222ra18.
23. Monti DA, Mitchell E, Bazzan AJ, Littman S, Zabrecky G, Yeo CJ, et al. Phase I evaluation of intravenous ascorbic acid in combination with gemcitabine and erlotinib in patients with metastatic pancreatic cancer. PLoS One. 2012; 7(1):e29794. [PubMed: 22272248]
24. Espey MG, Chen P, Chalmers B, Drisko J, Sun AY, Levine M, et al. Pharmacologic ascorbate synergizes with gemcitabine in preclinical models of pancreatic cancer. Free Radic Biol Med. Jun 1; 2011 50(11):1610–1619. [PubMed: 21402145]
25. Martinotti S, Ranzato E, Burlando B. In vitro screening of synergistic ascorbate-drug combinations for the treatment of malignant mesothelioma. Toxicol In Vitro. Dec; 2011 25(8):1568–1574. [PubMed: 21645609]
26. Hoffman NE, Chandramoorthy HC, Shamugapriya S, Zhang X, Rajan S, Mallilankaraman K, et al. MICU1 motifs define mitochondrial calcium uniporter binding and activity. Cell Rep. Dec 26; 2013 5(6):1576–1588. [PubMed: 24332854]
27. Beers RF Jr, Sizer IW. A spectrophotometric method for measuring the breakdown of hydrogen peroxide by catalase. J Biol Chem. Mar; 1952 195(1):133–140. [PubMed: 14938361]
28. Flohe L, Gunzler WA. Assays of glutathione peroxidase. Methods Enzymol. 1984; 105:114–121. [PubMed: 6727659]
29. Weydert CJ, Cullen JJ. Measurement of superoxide dismutase, catalase and glutathione peroxidase in cultured cells and tissue. Nat Protoc. Jan; 2010 5(1):51–66. [PubMed: 20057381]
30. Du J, Martin SM, Levine M, Wagner BA, Buettner GR, Wang S, et al. Mechanisms of Ascorbate-Induced Cytotoxicity in Pancreatic Cancer. Clinical Cancer Research. 2010; 16(2):509–520. [PubMed: 20068072]
31. Belousov VV, Fradkov AF, Lukyanov KA, Staroverov DB, Shakhbazov KS, Terskikh AV, et al. Genetically encoded fluorescent indicator for intracellular hydrogen peroxide. Nat Methods. Apr; 2006 3(4):281–286. [PubMed: 16554833]
32. Poburko D, Santo-Domingo J, Demaurex N. Dynamic regulation of the mitochondrial proton gradient during cytosolic calcium elevations. J Biol Chem. Apr 1; 2011 286(13):11672–11684. [PubMed: 21224385]
33. Mishina NM, Markvicheva KN, Bilan DS, Matlashov ME, Shirmanova MV, Liebl D, et al. Visualization of intracellular hydrogen peroxide with HyPer, a genetically encoded fluorescent probe. Methods Enzymol. 2013; 526:45–59. [PubMed: 23791093]
34. Csordas G, Hajnoczky G. Sorting of calcium signals at the junctions of endoplasmic reticulum and mitochondria. Cell Calcium. Apr; 2001 29(4):249–262. [PubMed: 11243933]
35. Pacher P, Sharma K, Csordas G, Zhu Y, Hajnoczky G. Uncoupling of ER-mitochondrial calcium communication by transforming growth factor-beta. Am J Physiol Renal Physiol. Nov; 2008 295(5):F1303–12. [PubMed: 18653477]
36. Szalai G, Krishnamurthy R, Hajnoczky G. Apoptosis driven by IP(3)-linked mitochondrial calcium signals. EMBO J. Nov 15; 1999 18(22):6349–6361. [PubMed: 10562547]
37. Ehrenberg B, Montana V, Wei MD, Wuskell JP, Loew LM. Membrane potential can be determined in individual cells from the nernstian distribution of cationic dyes. Biophys J. May; 1988 53(5): 785–794. [PubMed: 3390520]

38. Scaduto RC, Grotyohann LW. Measurement of Mitochondrial Membrane Potential Using Fluorescent Rhodamine Derivatives. Biophys J. 1999; 76(1):469–477. [PubMed: 9876159]
39. Farkas DL, Wei MD, Febbroriello P, Carson JH, Loew LM. Simultaneous imaging of cell and mitochondrial membrane potentials. Biophys J. Dec; 1989 56(6):1053–1069. [PubMed: 2611324]
40. Long LH, Evans PJ, Halliwell B. Hydrogen peroxide in human urine: implications for antioxidant defense and redox regulation. Biochem Biophys Res Commun. Sep 7; 1999 262(3):605–609. [PubMed: 10471371]
41. Rhee SG, Woo HA, Kil IS, Bae SH. Peroxiredoxin functions as a peroxidase and a regulator and sensor of local peroxides. J Biol Chem. Feb 10; 2012 287(7):4403–4410. [PubMed: 22147704]
42. Sies H. Role of Metabolic H2O2 Generation: Redox signaling and oxidative stress. J Biol Chem. 2014; 289(13):8735–8741. [PubMed: 24515117]
43. Feinstein RN, Berliner S, Green FO. Mechanism of inhibition of catalase by 3-amino-1,2,4-triazole. Arch Biochem Biophys. 1958; 76(1):32–44. [PubMed: 13560010]
44. Schallreuter KU, Gleason FK, Wood JM. The mechanism of action of the nitrosourea anti-tumor drugs on thioredoxin reductase, glutathione reductase and ribonucleotide reductase. Biochim Biophys Acta. Aug 13; 1990 1054(1):14–20. [PubMed: 2200526]
45. Halliwell, B.; Whiteman, M. Antioxidant and Prooxidant Properties of Vitamin C.. In: Packer, L.; Fuchs, J., editors. Vitamin C in Health and Disease New York. Marcel Dekker, INC.; New York: 1997. p. 59
46. Savini I, Rossi A, Pierro C, Avigliano L, Catani MV. SVCT1 and SVCT2: key proteins for vitamin C uptake. Amino Acids. Apr; 2008 34(3):347–355. [PubMed: 17541511]
47. Yun J, Mullarky E, Lu C, Bosch KN, Kavalier A, Rivera K, et al. Vitamin C selectively kills KRAS and BRAF mutant colorectal cancer cells by targeting GAPDH. Science. Dec 11; 2015 350(6266): 1391–1396. [PubMed: 26541605]
48. Chen Q, Vazquez EJ, Moghaddas S, Hoppel CL, Lesnefsky EJ. Production of reactive oxygen species by mitochondria: central role of complex III. J Biol Chem. Sep 19; 2003 278(38):36027–36031. [PubMed: 12840017]
49. Murphy MP. How mitochondria produce reactive oxygen species. Biochem J. Jan 1; 2009 417(1): 1–13. [PubMed: 19061483]
50. Fleury C, Mignotte B, Vayssiere JL. Mitochondrial reactive oxygen species in cell death signaling. Biochimie. Feb-Mar;2002 84(2-3):131–141. [PubMed: 12022944]
51. Orrenius S. Reactive oxygen species in mitochondria-mediated cell death. Drug Metab Rev. 2007; 39(2-3):443–455. [PubMed: 17786631]
52. Winterbourn CC. The challenges of using fluorescent probes to detect and quantify specific reactive oxygen species in living cells. Biochim Biophys Acta. Feb; 2014 1840(2):730–738. [PubMed: 23665586]
53. Choi H, Kim S, Mukhopadhyay P, Cho S, Woo J, Storz G, et al. Structural basis of the redox switch in the OxyR transcription factor. Cell. Apr 6; 2001 105(1):103–113. [PubMed: 11301006]
54. Lee C, Lee SM, Mukhopadhyay P, Kim SJ, Lee SC, Ahn WS, et al. Redox regulation of OxyR requires specific disulfide bond formation involving a rapid kinetic reaction path. Nat Struct Mol Biol. Dec; 2004 11(12):1179–1185. [PubMed: 15543158]
55. Bogeski I, Kappl R, Kummerow C, Gulaboski R, Hoth M, Niemeyer BA. Redox regulation of calcium ion channels: chemical and physiological aspects. Cell Calcium. Nov; 2011 50(5):407–423. [PubMed: 21930299]
56. Yan Y, Wei CL, Zhang WR, Cheng HP, Liu J. Cross-talk between calcium and reactive oxygen species signaling. Acta Pharmacol Sin. Jul; 2006 27(7):821–826. [PubMed: 16787564]
57. McCubrey JA, Steelman LS, Chappell WH, Abrams SL, Wong EW, Chang F, et al. Roles of the Raf/MEK/ERK pathway in cell growth, malignant transformation and drug resistance. Biochim Biophys Acta. Aug; 2007 1773(8):1263–1284. [PubMed: 17126425]
58. Roberts PJ, Der CJ. Targeting the Raf-MEK-ERK mitogen-activated protein kinase cascade for the treatment of cancer. Oncogene. May 14; 2007 26(22):3291–3310. [PubMed: 17496923]
59. Zhang W, Liu HT. MAPK signal pathways in the regulation of cell proliferation in mammalian cells. Cell Res. Mar; 2002 12(1):9–18. [PubMed: 11942415]

60. Chou TC. Theoretical basis, experimental design, and computerized simulation of synergism and antagonism in drug combination studies. Pharmacol Rev. Sep; 2006 58(3):621–681. [PubMed: 16968952]

61. Bull VH, Rajalingam K, Thiede B. Sorafenib-induced mitochondrial complex I inactivation and cell death in human neuroblastoma cells. J Proteome Res. Mar 2; 2012 11(3):1609–1620. [PubMed: 22268697]

62. Tesori V, Piscaglia AC, Samengo D, Barba M, Bernardini C, Scatena R, et al. The multikinase inhibitor Sorafenib enhances glycolysis and synergizes with glycolysis blockade for cancer cell killing. Scientific Reports. 2015; 5:9149. [PubMed: 25779766]

63. Oberley TD, Oberley LW. Antioxidant enzyme levels in cancer. Histol Histopathol. Apr; 1997 12(2):525–535. [PubMed: 9151141]

64. Aruoma OI, Halliwell B. Superoxide-dependent and ascorbate-dependent formation of hydroxyl radicals from hydrogen peroxide in the presence of iron. Are lactoferrin and transferrin promoters of hydroxyl-radical generation? Biochem J. Jan 1; 1987 241(1):273–278. [PubMed: 3032157]

65. Buettner GR. Ascorbate autoxidation in the presence of iron and copper chelates. Free Radic Res Commun. 1986; 1(6):349–353. [PubMed: 2851502]

66. Zaidi A, Barron L, Sharov VS, Schoneich C, Michaelis EK, Michaelis ML. Oxidative inactivation of purified plasma membrane Ca2+-ATPase by hydrogen peroxide and protection by calmodulin. Biochemistry. Oct 21; 2003 42(41):12001–12010. [PubMed: 14556631]

67. Plecita-Hlavata L, Lessard M, Santorova J, Bewersdorf J, Jezek P. Mitochondrial oxidative phosphorylation and energetic status are reflected by morphology of mitochondrial network in INS-1E and HEP-G2 cells viewed by 4Pi microscopy. Biochim Biophys Acta. Jul-Aug;2008 1777(7-8):834–846. [PubMed: 18452700]

68. Li X, Cobb CE, May JM. Mitochondrial recycling of ascorbic acid from dehydroascorbic acid: dependence on the electron transport chain. Arch Biochem Biophys. Jul 1; 2002 403(1):103–110. [PubMed: 12061807]

Highlights

- Ascorbate in pharmacologic dose kills tumor cells by potentiating H_2O_2 cytotoxicity
- Ascorbate and sorafenib exhibit synergistic cytotoxicity in Hep G2 cells
- Ascorbate deregulates cellular Ca^{2+} homeostasis causing mitochondrial Ca^{2+} overload
- Sorafenib depolarizes mitochondria exacerbating ascorbate-induced Ca^{2+} deregulation
- Regression of rib metastasis in HCC patient treated with ascorbate and sorafenib

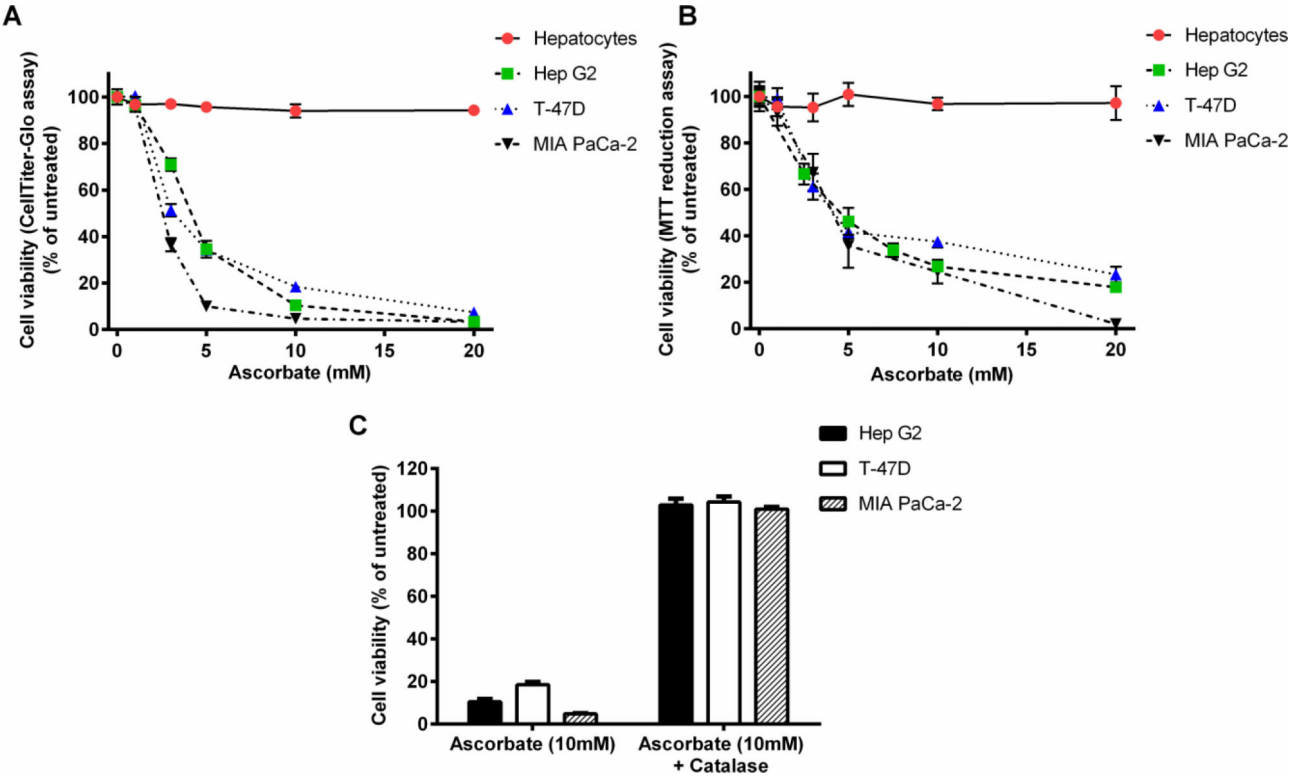

Figure 1. Ascorbate induces cytotoxicity in cancer cells, but not in primary hepatocytes

Cell viability was measured using either the CellTiter-Glo® Luminescent cell viability assay (Promega) (A and C) or the MTT assay (B) after two hour treatment with various concentrations of ascorbate (1, 3, 5, 10, or 20 mM) (A and B) and the addition of catalase (100 μg/mL) to the media (C). Error bars represent the SEM (n=3). Some error bars may be smaller than the symbol.

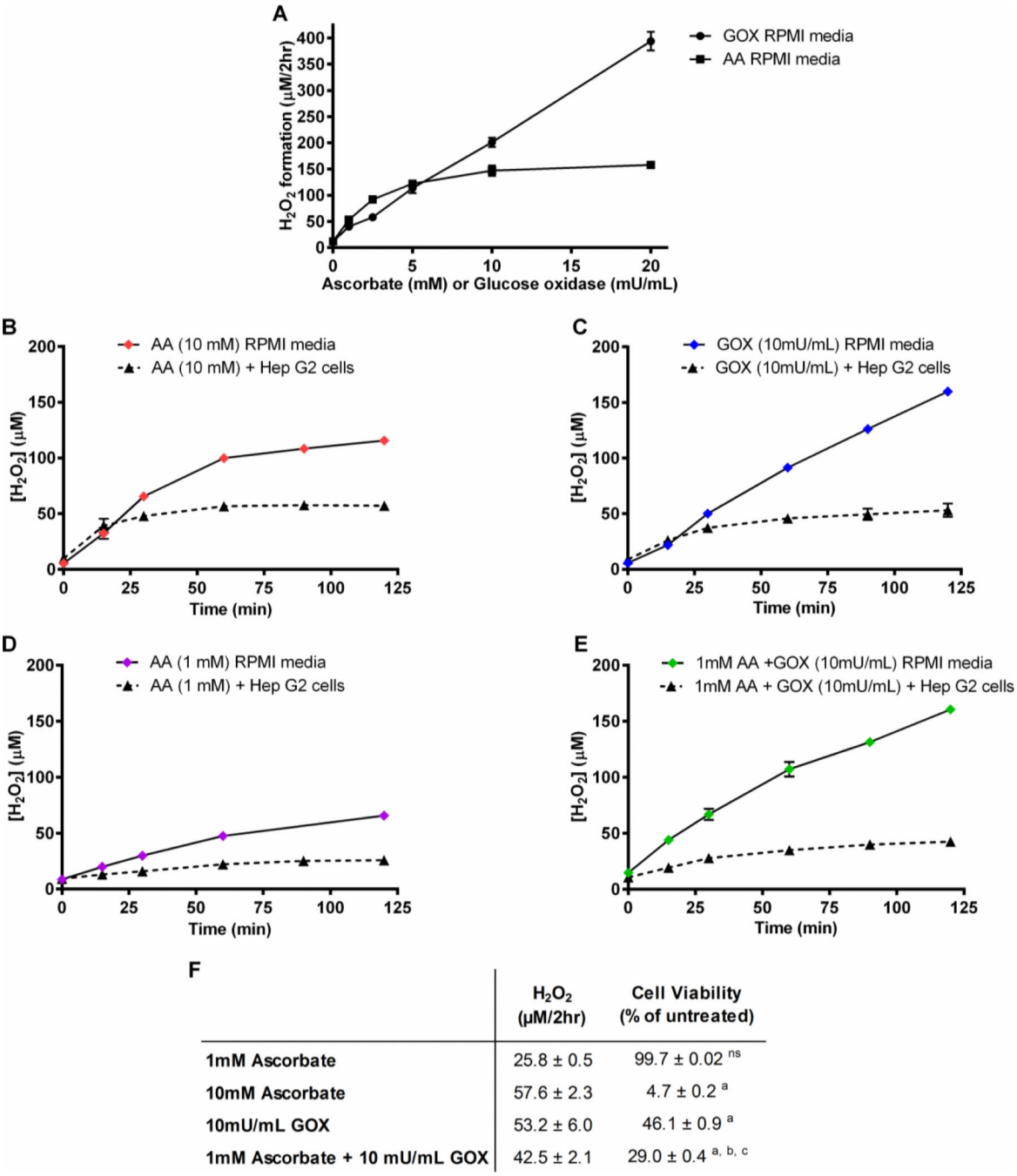

F

	H_2O_2 (μM/2hr)	Cell Viability (% of untreated)
1mM Ascorbate	25.8 ± 0.5	99.7 ± 0.02 [ns]
10mM Ascorbate	57.6 ± 2.3	4.7 ± 0.2 [a]
10mU/mL GOX	53.2 ± 6.0	46.1 ± 0.9 [a]
1mM Ascorbate + 10 mU/mL GOX	42.5 ± 2.1	29.0 ± 0.4 [a, b, c]

Figure 2. H_2O_2 formation by ascorbate and GOX in the absence and presence of Hep G2 cells

(A) Various concentrations of ascorbate or GOX were added to RPMI 1640 media without cells and H_2O_2 formation was measured over a 2 hour period using a Clark Electrode. (B-E) Time course of H_2O_2 formation upon addition of 10 mM ascorbate (B), 10 mU/mL GOX (C), 1 mM ascorbate (D), or 10 mU/mL GOX + 1 mM ascorbate (D), added to RPMI 1640 media in the absence or presence of Hep G2 cells. (F) Comparison of steady state concentrations of H_2O_2 and cell viability after 2 hrs of incubation of HepG2 cells with 1 mM ascorbate, 10mM ascorbate, 10 mU GOX/mL, or 1mM ascorbate + 10mU GOX/mL. ns

– not significant compared to untreated, a - $p<0.0001$ compared to untreated, b – $p<0.0001$ compared to 10mU/mL GOX, c – $p<0.0001$ compared to 1mM ascorbate. AA = ascorbate, GOX = glucose oxidase. Some error bars may be smaller than the symbol.

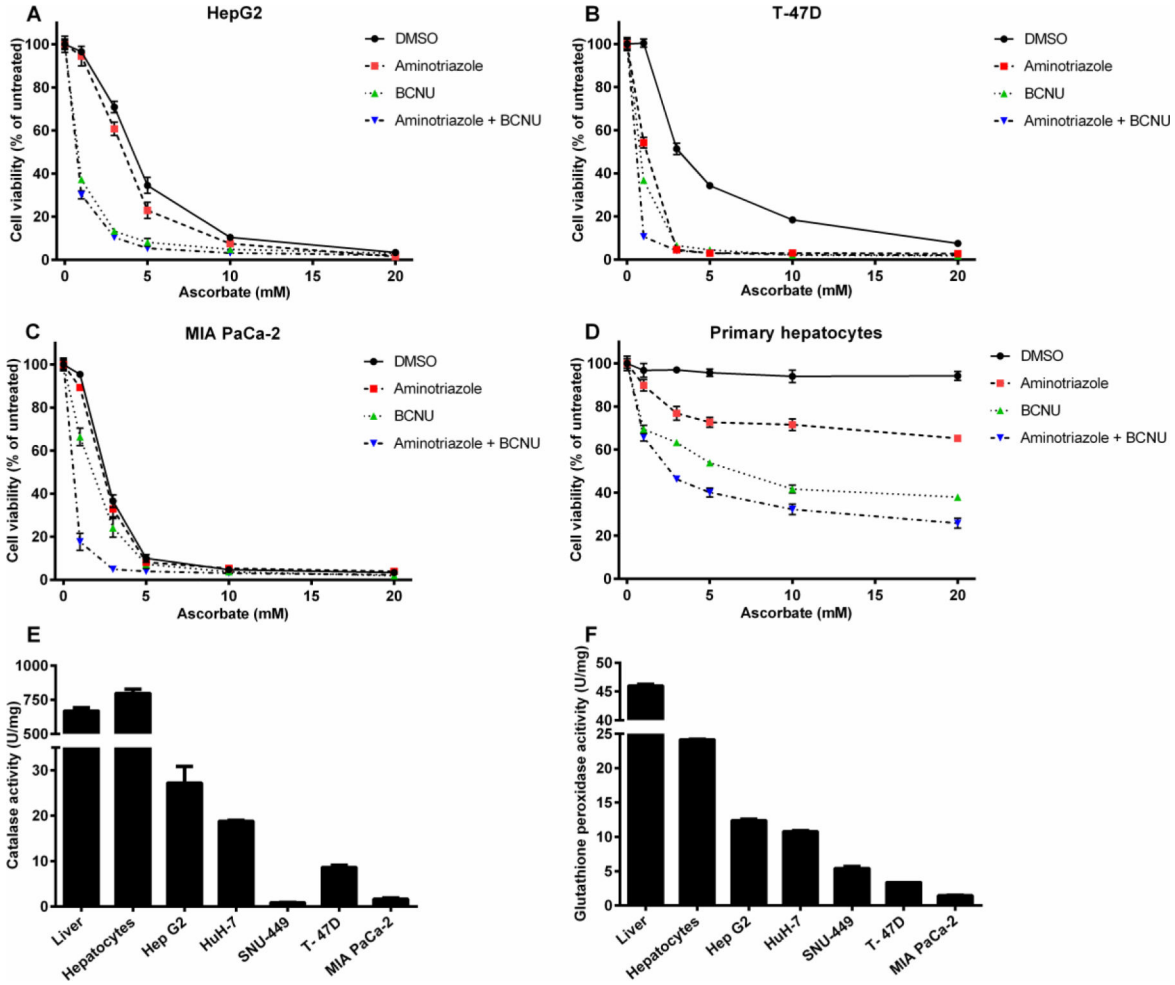

Figure 3. Inhibition of antioxidant enzymes sensitizes cancer cell lines and primary hepatocytes to ascorbate mediated cytotoxicity

Hep G2 cells (A), T-47D cells (B), MIA PaCa-2 cells (C), and primary hepatocytes (D) were preincubated for one hour with no inhibitors, the catalase inhibitor 3-amino-1,2,4-triazole (AT) (5 mM), the glutathione reductase/thioredoxin reductase inhibitor BCNU/carmustine (100 μM), or both inhibitors, followed by a two hour treatment with different concentrations of ascorbate (1, 3, 5, 10, and 20 mM). Cell viability was measured through CellTiter-Glo cell viability assay. Error bars represent SEM (n=3). Activity levels of catalase (E) and Glutathione peroxidase (F) in rat liver tissue, primary rat hepatocytes, Hep G2, Huh-7, SNU-449, T-47D, and MIA PaCa-2 cells. Error bars represent SEM (n=4). Some error bars may be smaller than the symbol.

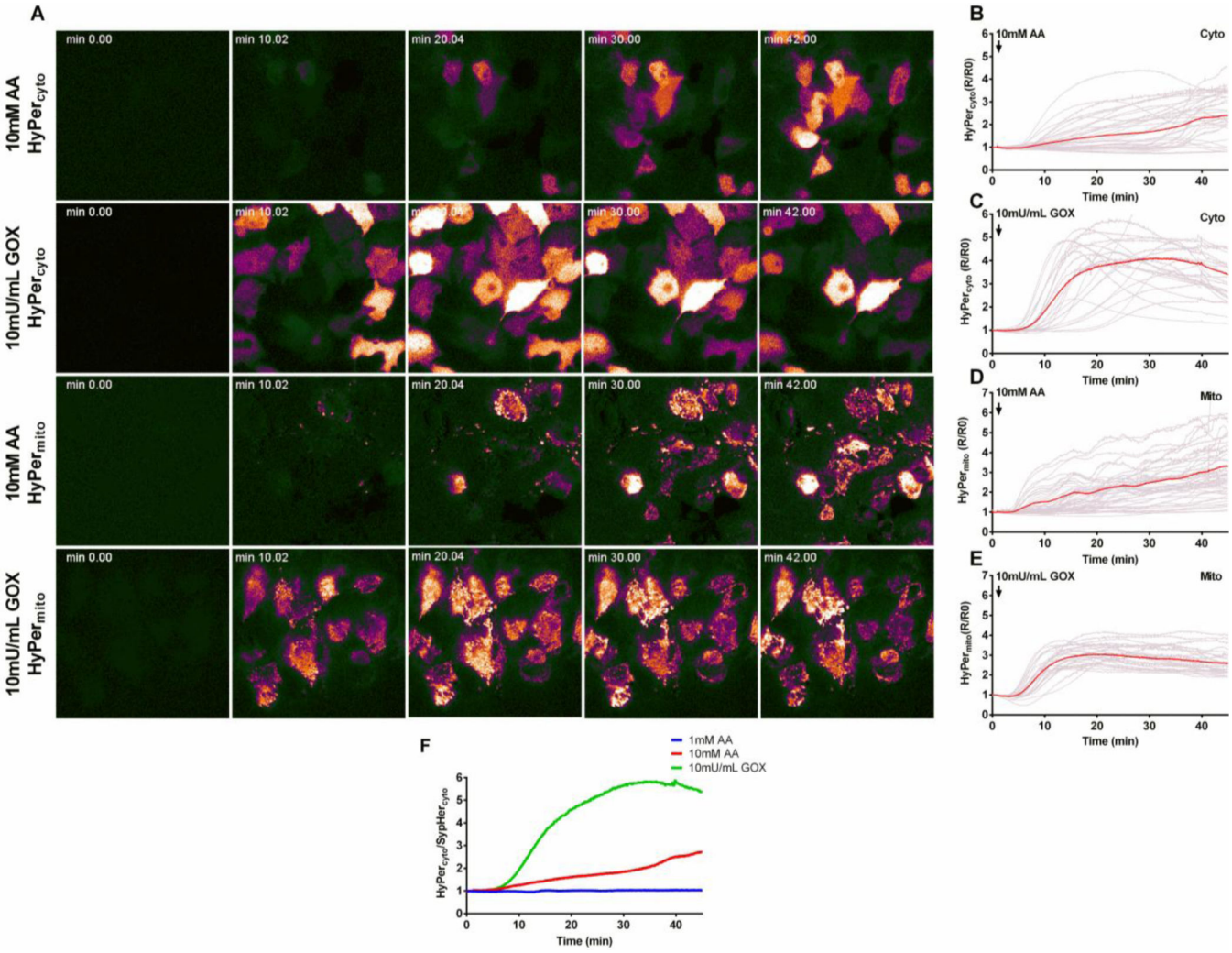

Figure 4. Intracellular H_2O_2 in the cytosol and mitochondrial matrix of Hep G2 cells after treatment with ascorbate or GOX using the genetically encoded sensor HyPer as a probe

Hep G2 cells were transfected with HyPer$_{cyto}$ or HyPer$_{mito}$ as described in Materials and Methods. (A) Time course of HyPer$_{cyto}$ and HyPer$_{mito}$ fluorescence ratio after treatment with 10 mM ascorbate (first and third rows) or 10 mU/mL GOX (second and fourth rows). (B-C) Ratiometric fluorescent traces of individual cells expressing HyPer$_{cyto}$ after treatment with 10 mM ascorbate (B) or 10 mU/mL GOX (C). Red traces represent average fluorescence intensity over all cells (D-E) Ratiometric fluorescence traces of individual cells expressing HyPer$_{mito}$ after treatment with 10 mM ascorbate (D) or 10 mU/mL GOX (E). (F) Ratio of average HyPer$_{cyto}$ to SypHer$_{cyto}$ fluorescence signals after treatment with 1 mM ascorbate (blue), 10 mM ascorbate (red), or 10 mU/mL GOX (green). AA = ascorbate, GOX = glucose oxidase.

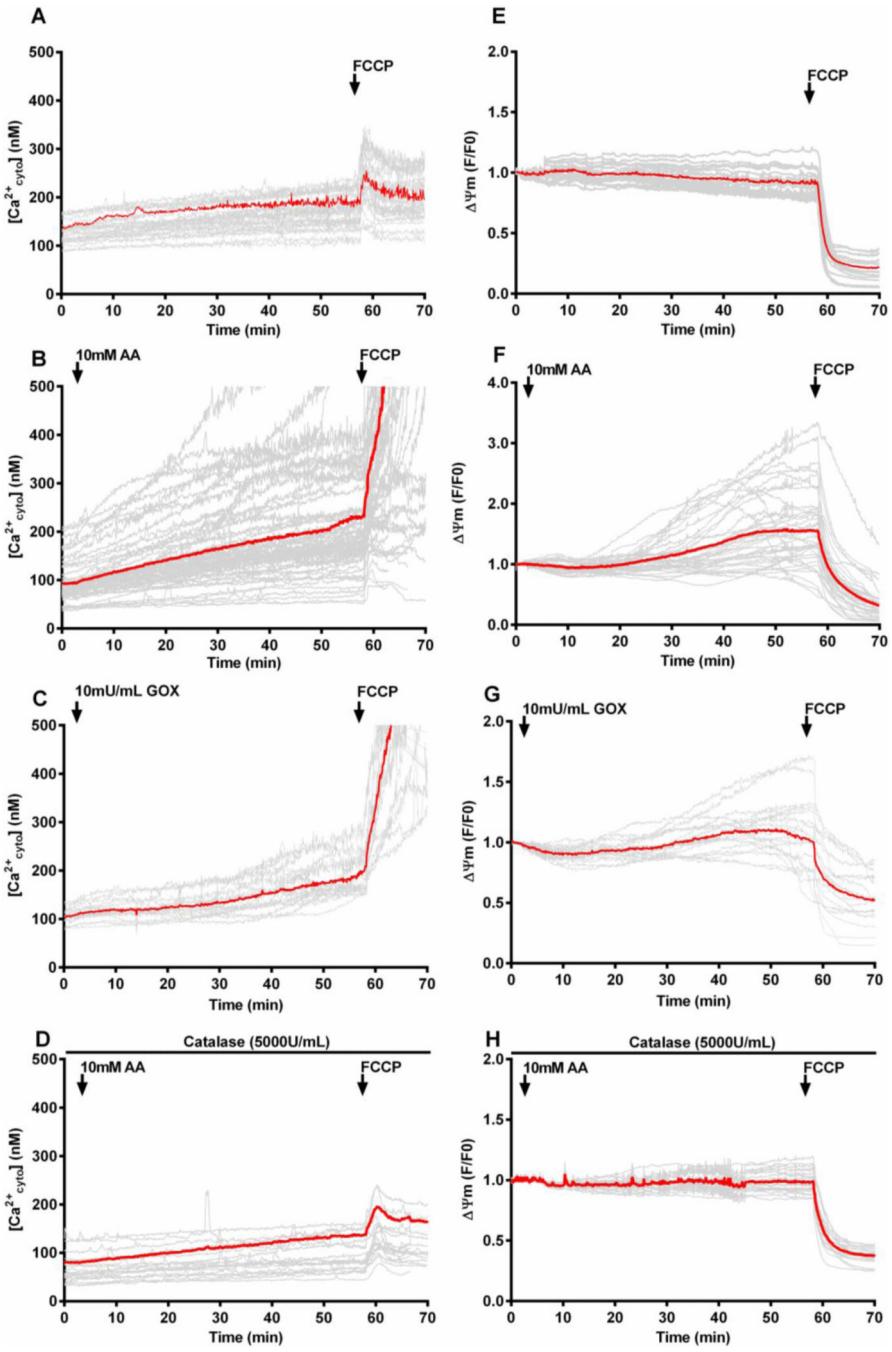

Figure 5. Cytosolic calcium and mitochondrial membrane potential measurements in Hep G2 cells after ascorbate or GOX addition

(A-D) Time course of cytosolic calcium [Ca^{2+}_{cyto}] changes recorded using Fura-2 in intact Hep G2 cells with no additions (A), ascorbate (10 mM) (B), GOX (10 mU/mL) (C), or ascorbate (10 mM) plus catalase (100 μg/mL) (D). (E-H) Time course of mitochondrial membrane potential changes measured in parallel incubations by TMRE fluorescence. For all traces, an addition of FCCP (5 μM) was made at approximately 60 minutes as indicated by an arrow. Red traces represent average fluorescence intensity over all cells (n=15-30). AA= ascorbate, GOX= glucose oxidase

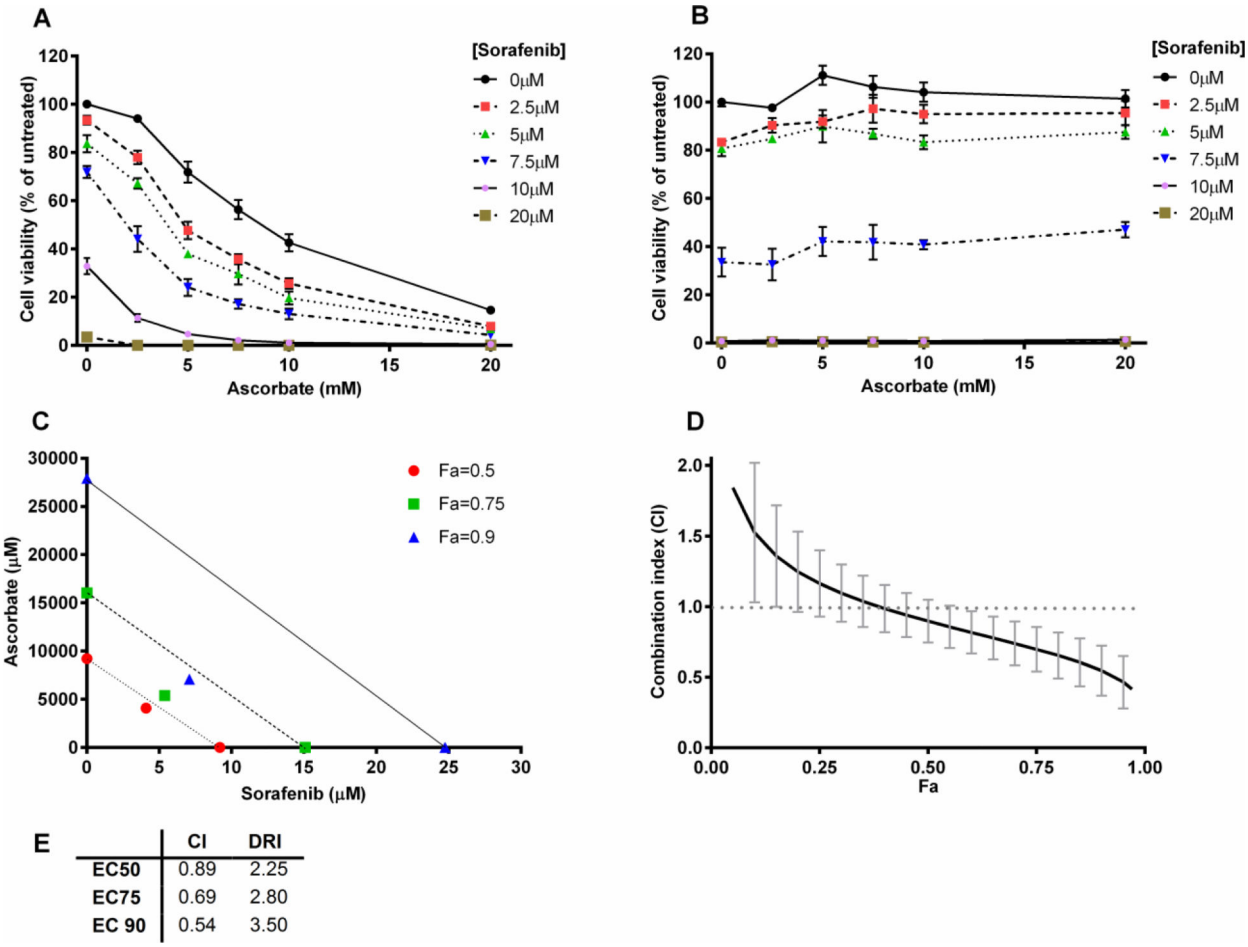

E

	CI	DRI
EC50	0.89	2.25
EC75	0.69	2.80
EC 90	0.54	3.50

Figure 6. Synergistic cell killing after combination treatment with ascorbate and sorafenib

Hep G2 cells (A) or primary hepatocytes (B) were preincubated with various concentrations of sorafenib (2.5, 5, 7.5, 10, and 20 μM) for 20 hours prior to treatment with various concentrations of ascorbate (2.5, 5, 7.5, 10, and 20 mM) for 2 hours. Viability was measured using the CellTiter-Glo cell viability assay. Error bars represent the SEM (n=3 and n=1 for A and B respectively). (C) An isobologram constructed from the calculation of the combination index (CI), Fa = fraction affected. (D) Serial deletion analysis to calculate 95% confidence intervals of the CI (n=3). (E) Calculated values of the CI and dose reduction index (DRI) at different effective concentration (EC) levels. (C-E) Values were based on the Chou-Talalay method using the CompuSyn software with a constant ratio of doses. Some error bars may be smaller than the symbol.

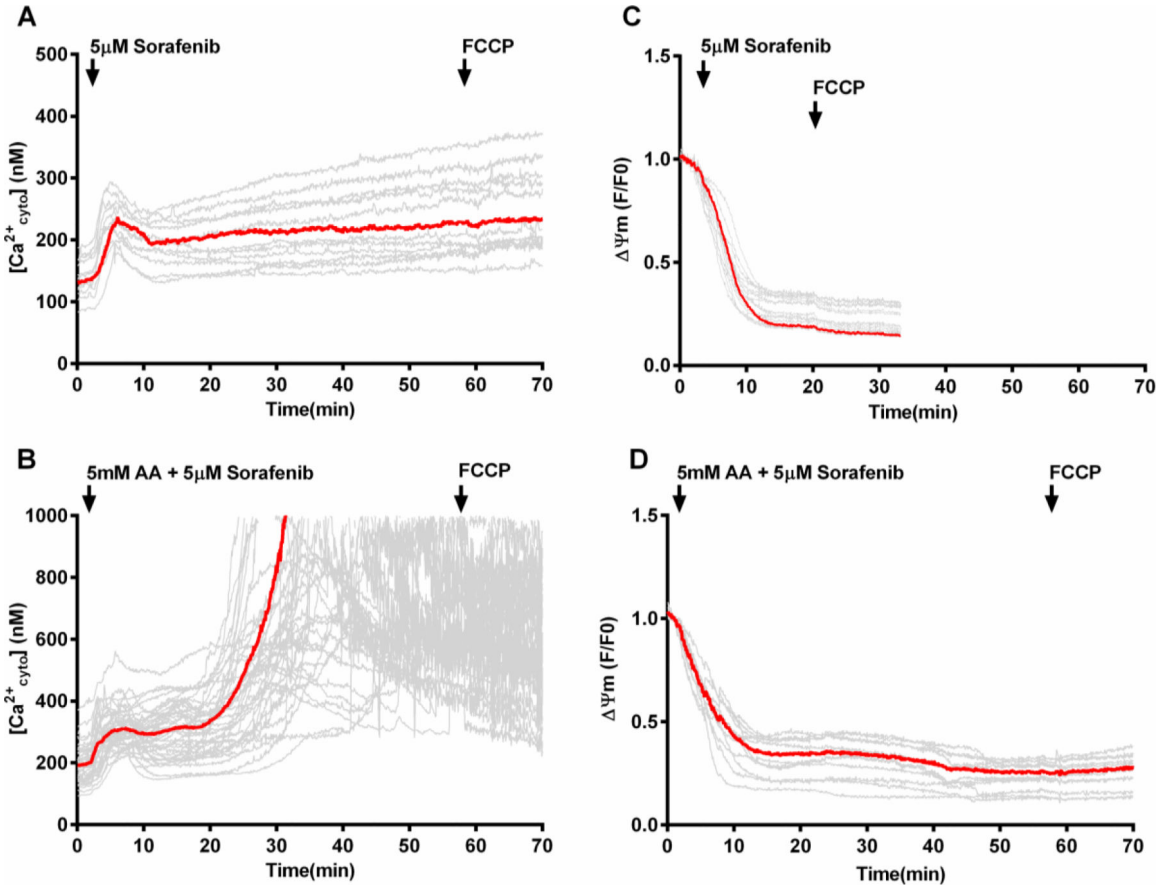

Figure 7. Cytosolic calcium and mitochondrial membrane potential changes in Hep G2 cells after treatment with sorafenib or the combination of ascorbate and sorafenib

Time course of $[Ca^{2+}_{cyto}]$ recorded in Hep G2 cells loaded with Fura-2 and, in separate incubations, mitochondrial membrane potentials recorded in Hep G2 cells loaded with TMRE, upon treatment with sorafenib (5 μM) (A and C) or the combination of ascorbate (5 mM) and sorafenib (5μM) (B and D). Arrow indicates addition of 5 μM FCCP. Red traces represent average fluorescence intensity over all cells. (n=15-30). AA, ascorbate.

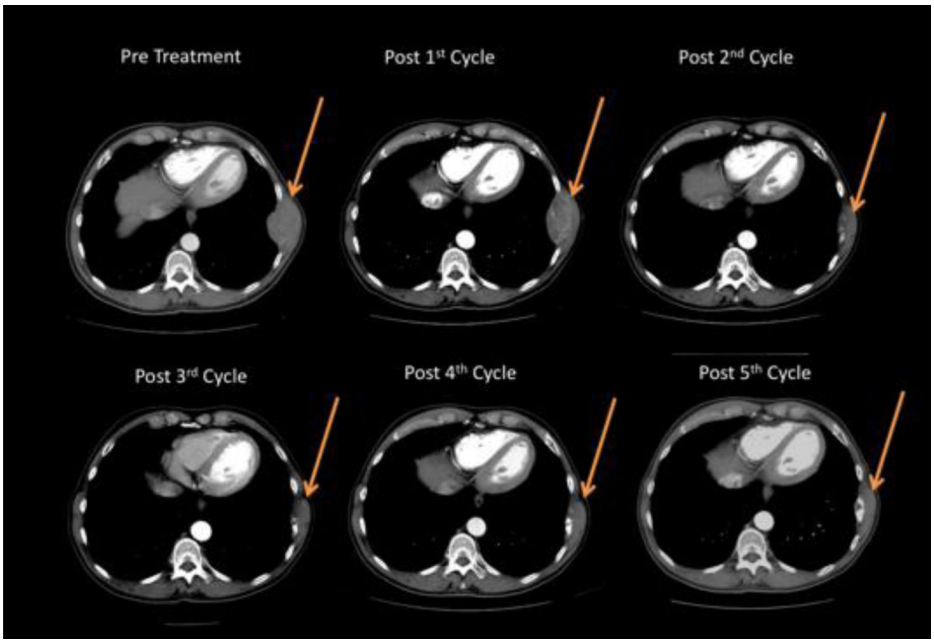

Figure 8. Computed tomography scan of case study patient who experienced a metastatic tumor regression during treatment with the combination of ascorbate and sorafenib

Transverse CT image of a patient with HCC. Arrow indicates a rib metastasis.